

University of New South Wales
Graduate School of Biomedical Engineering
Non-Plagiarism Declaration

z5209029	Najdzion	Joshua
----------	----------	--------

Student Number

Family Name

Other Names

BIOM4953	Research Thesis C
----------	-------------------

Course ID

Course Name

22/11/2021	Michael Stevens
------------	-----------------

Submission Date

Course Coordinator/Lecturer

Final Thesis - Multi Objective optimisation of Stents


Assignment Title

In preparing this assessment task I have followed the [Student Code of Conduct](#). I certify that I have read and understand the University requirements in respect of student academic misconduct outlined in the [Student Code of Conduct](#) and the [Student Misconduct Procedures](#), and am aware of any potential plagiarism penalties which may apply. I declare that this assessment item is my own work except where acknowledged, and has not been submitted for academic credit previously in whole or in part. If this is part of a group submission, it represents my equitable contribution and is my own work, except where appropriately acknowledged.

I acknowledge that the assessor of this item may, for assessment purposes:

- Provide a copy to another staff member of the University.
- Communicate a copy of this assessment item to a plagiarism checking service (such as [Turnitin](#)) which may then retain a copy of the assessment item on its database for the purpose of future plagiarism checking.

I have retained a copy of this, my assignment, which I can provide if necessary. By signing this declaration I am agreeing to the statements and conditions above.

	22/11/2021
---	------------

Signature

Date



Graduate School of Biomedical Engineering

Faculty of Engineering

University of New South Wales

Multi-Objective Optimisation of Stents

Final Report

Author: Joshua Najdzion

zID:Z5209029

Coronary artery disease is a leading cause of cardiovascular related deaths, with stents often providing symptomatic relief. Although stents have seen much use, they continue to see problems that hinder their performance. This investigation aims to improve this by analysing material selection. Methods included performing simulations for bending, longitudinal compression and radial compression as well as using optimisation code to generate new stent designs across a large range of materials. Results have shown a stiffness ranking in which stiffer materials, traditionally considered to yield better performance, may not necessarily provide optimal results in a range of tests. This has brought forth the potential for alternate material choices, revealing now further investigation to be undertaken. This novel examination of stent materials and their crucial role in stent design examined all aspects to begin to grasp the multi-faceted aspects of stent design and how a myriad of parameters affect their performance.

Acknowledgements

I would like to express my gratitude to my thesis supervisor Dr Susann Beier for her continual guidance, critiques, and support throughout the duration of my thesis. I would also like to acknowledge Mr Ramtin Gharleghi for assisting in setting up various simulations and quick responses. His expertise on CFD simulations and the optimisation code was an invaluable assistance to this project, especially when starting out. Additionally, I would like to thank Vanessa Luvio for creating the robust base FEA tests that were used in my thesis. Further, her instructions on using this software were highly informative and were of great help. I would also like to thank Deepan Kumar for assisting with computational issues and CFD set up. Finally, I would like to thank Alexander Cunio for his continued support and assistance throughout the thesis.

Statement Of Contribution

Throughout this thesis, the work was undertaken by multiple individuals including myself. Such tasks included base files used, the completed work and final analysis.

Ramtin Gharleghi among others have helped form the optimisation code to its current form in which I used the software but have not aided to its development.

Vanessa Luvio created base FEA and CFD files that were used in my thesis as is or as a starting point where errors were fixed, or aspects were changed.

The previous geometries that were used in the initial simulations were created by Vanessa Luvio using the optimisation code. The new stents that were generated were created by myself using a stent geometry script made by others.

All data in the FEA and CFD testing was obtained by myself using Katan and all analysis and post processing was undertaken by myself.

Contents

Acknowledgements	ii
Statement Of Contribution	ii
1. Introduction	1
1.1. Background	1
1.2. Design of Stents	2
1.3. Failure of Stents	3
1.3.1. In Stent Restenosis	4
1.3.2. Stent Thrombosis	4
1.4. Aims	6
2. Chapter 2 – Literature Review	7
2.1. Evolution of Stents	7
2.2. Ideal Stent Properties	9
2.3. Current Materials	12
2.4. Finite Element Analysis	15
2.5. Experimental Testing	18
2.6. Computational Fluid Dynamics	19
2.7. Motivation For Research	19
3. Methodology	20
3.1. Overview	20
3.2. Stent Geometry	22
3.3. Materials	23
3.4. Mechanical Testing	24
3.4.1. Compression	25
3.4.2. Bending	27
3.4.3. Radial Compression	28
3.5. Multi- Objective Optimisation process	31
4. Results	33
4.1. Finite Element Analysis – Base Results	33
4.2. Multi Objective Optimisation Process	38

5.	Discussion	44
6.	Future Work	47
7.	Conclusion	49
8.	References.....	50
9.	Appendices.....	54
9.1.	Appendix A.....	54
9.2.	Appendix B	64
9.3.	Appendix C	67

1. Introduction

1.1. Background

Coronary artery disease (CAD) accounted for 11% of deaths in Australia between 2017 and 2018 [1], making it the leading cause of death in Australia. This disease occurs from a build-up of plaque within blood vessels, a substance made up from cholesterol. This can cause the arteries to narrow over a long period of time which has the capacity to lower or block the blood flow to vital organs, having the ability to decrease various bodily functions and even lead to death.

The development of the stent which is a mesh implanted within obstructed blood vessels to restore blood flow has seen a reduction in the effects of CAD, improving patients' overall quality of life. However, there are multiple persisting problems associated with stents and improvements can still be made to increase performance stents and minimise the risks associated with their use.

The precursor to the stent was balloon angioplasty in which a balloon is inserted into the artery and expanded to re-open the artery and displace the plaque that is on the wall of the artery. Primary issues of this were restenosis, a narrowing of the blood vessel due to elastic recoil which was evident in 5-10% of operations [2] as well as the potential to tear an artery. Due to the myriad and severity of complications and shortness of resolution, the stent was designed as a superior alternative that could act as a longer lasting solution. From this, balloon angioplasty was re-developed into percutaneous coronary intervention (PCI) which is a combination of balloon angioplasty and using the balloon to insert and place the stent in the region of concern.

PCI was first developed in 1964 by Dotter and Judkins and later implemented in 1977 by Andreas Gruntzig [2], with the stent itself being first implanted in a patient in 1986 by Sigwart and Puel. Initially these were bare metal stents composed of various metals, most commonly stainless steel due to its biocompatibility and mechanical strength [3]. Stents became common place in 1993 when two trials established coronary stent implantation, making PCI a common procedure and an accepted standard of care.

The stent has rapidly evolved in its short time in use but still faces performance issues and can cause in stent restenosis and stent thrombosis, exemplified further in the following sections.

1.2. Design of Stents

The design of a stent is comprised of many variables and can be generally broken down into the structure of the stent or the choice of material. The material choice is dependent on the properties that are required by the design, interactions that occur with the body, and by other requirements including if it is required to have a drug coating or be bioresorbable.

Stent Structure

Stent structure is the result of the interplay of multiple factors, including the number of peaks in a ring, the number of rings as well as the number of connectors within the overall structure. Focusing on the peaks, the strut length is also a factor to be considered that affects the effective surface area and hence performance. Depending on the material chosen and the forces that are expected to be exerted on the design, the strut thickness can be designed with thinner struts allowing for a more flexible structure, however, thicker struts can resist higher levels of stress once deployed. Other such factors to be determined include the strut spacing and the ring amplitude [4] which can alter many performance factors in the stent. Figure 1 illustrates how all these design variables affect the stent geometry and how closely linked all parameters are.

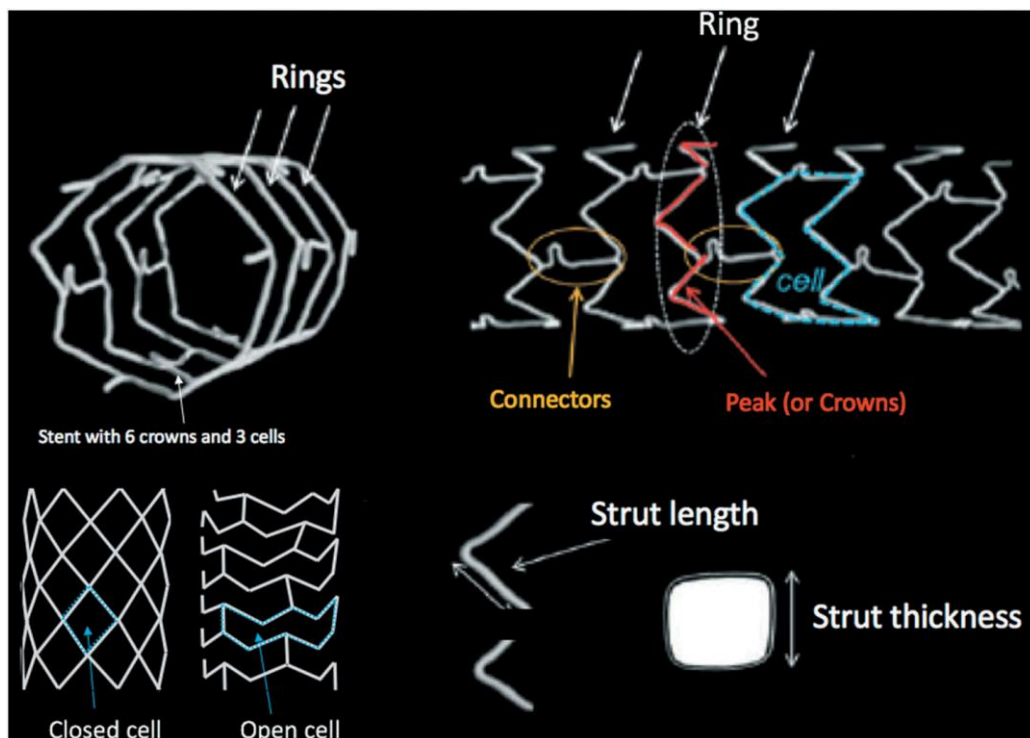


Figure 1. Basic Stent Structures and Stent Design Nomenclature [5]

Stent Material

Performance of a stent is highly attributed to the material used. Initially being comprised of stainless steel, materials these days can have unique properties and be specifically chosen for certain designs or situations. Currently, alloys are commonly used to deliver certain desirable properties whilst biodegradable materials are less mechanically strong but degrade in a lesser amount of time [5], proving to be useful in certain applications and minimised the occurrence of long term effects. Materials that perform better than conventional materials allow for stent designs to be less conservative and hence less material to be used.

1.3. Failure of Stents

There are multiple factors that contribute to the failure of stents, affected by both the design and material choice that can cause a mixture of mechanical failure or corrosion and fatigue. This is often not attributed to a single mode of failure but is a combination of multiple factors that come into play to enable the overall failure of the stent.

The mechanical failure can be related to a multitude of factors including axial and radial compression or extension as well as bending and torsion, which is exhibited over extended periods of time with consistent activity. Axial forces occur along the main body axis and allow the stent to be lengthened and compressed in a straight line [6]. Radial forces occur along the radius and are more often in compression due to the stent keeping the blood vessel open. If the stents radial expansion is too high, then it can cause the vessel to overexpand leading to injury [5]. Flexibility of a stent is inversely proportional to the bending stiffness and in general, stents perform worse in radial bending [7]. This property is a requirement of stents as they are often required to be placed in areas where the path is not straight and quite curved. The stents have to be flexible enough to reach the destination without surpassing the yield stress so that they are not plastically deformed before being deployed [8].

Other factors that can lead to failure include stent recoil, occurring when the balloon is inserted, and the stent is expanded yet reduces in radial size when the apparatus is removed, reducing its effectiveness. Stent recoil has also been known to be a long term issue that occurs over a period of time [9]. The radial strength of the stent is thought to be an indicator of how it will perform in this regard. Performance itself is not solely based on one attribute and requires multiple properties to be optimised so that the stent does not fail prematurely. Although it was originally thought that stiffer materials would perform

well in this regard, studies performed by Kitahara et al. [10, 11] have determined that less stiff materials can perform just as well if not better than conventionally used stiff materials.

1.3.1. In Stent Restenosis

One of the main problems associated with stents is in stent restenosis, a condition that results in the loss of luminal size after a intravascular procedure [12]. From this, the treated artery can become blocked again which usually occurs within 6 months of the original implantation [13]. Restenosis that occurs after a stent is implanted is called in stent restenosis (ISR). ISR forms when the stent is implanted and tissue grows over the stent, enabling a lower flow of blood (illustrated in Figure 3). Over time, scar tissue can form underneath the endothelium which leads to blockages in the artery. Studies have shown restenosis rates before stents was as high as 55%, whilst bare metal stents have lowered it to 17-41% and finally drug eluting stents have lowered this number to <10% [14]. Nonetheless, restenosis remains a large issue for stents that must be overcome, requiring further modification to both the material and design choices for the stent itself.

1.3.2. Stent Thrombosis

In contrast to in stent restenosis, stent thrombosis occurs when there is a thrombotic occlusion in the vessel [15]. Often this is a blood clot, which can cause lead to high rates of morbidity and mortality. Further causes of stent thrombosis are outlined within Figure 2. Stent thrombosis can occur both in very short and long-time spans ranging from 24 hours to over 12 months [16]. A dated test performed by Mauri et al. [17] determined that drug eluting stents (DES) didn't lower the rate of stent thrombosis but did lower the rates of restenosis. Torrado et al. [18] found in 2018 that thinner struts may lower stent thrombosis, however DES stents have not yet minimised the risk of thrombosis. Both restenosis and thrombosis can cause serious consequences and whilst in stent restenosis has less occurrence in the modern day, thrombosis is still a challenge with material selection potentially being a key factor to overcome some of the effects and increase the longevity for the patients.

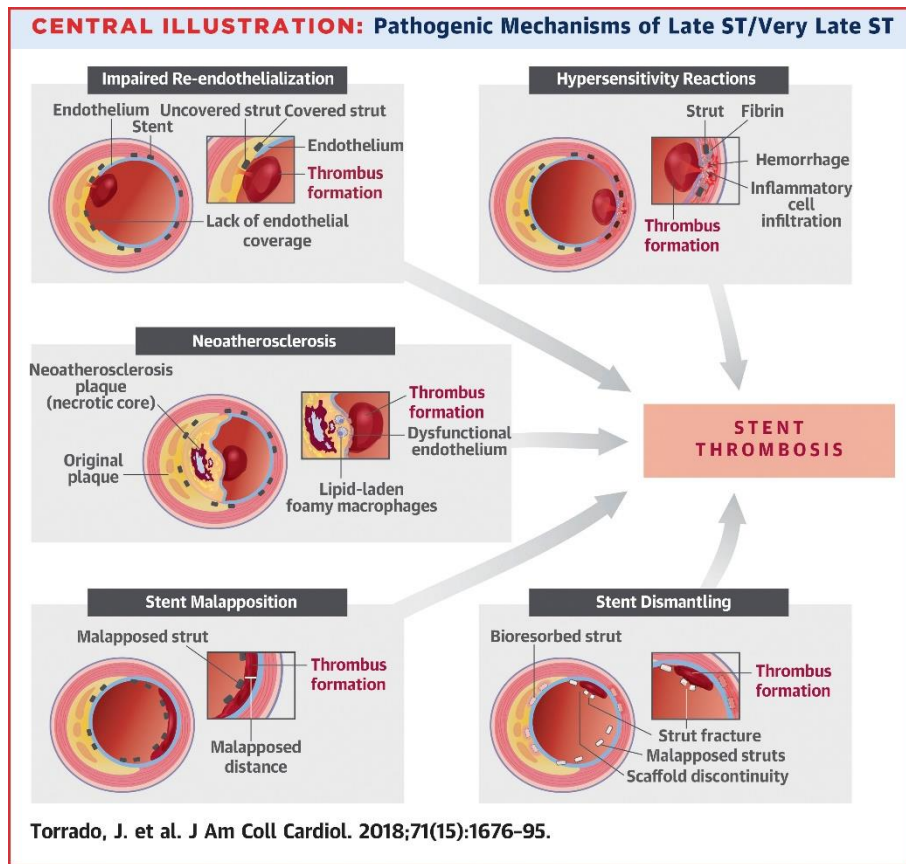


Figure 2. Pathogenic Mechanisms of Late ST/ Very Late ST [18]

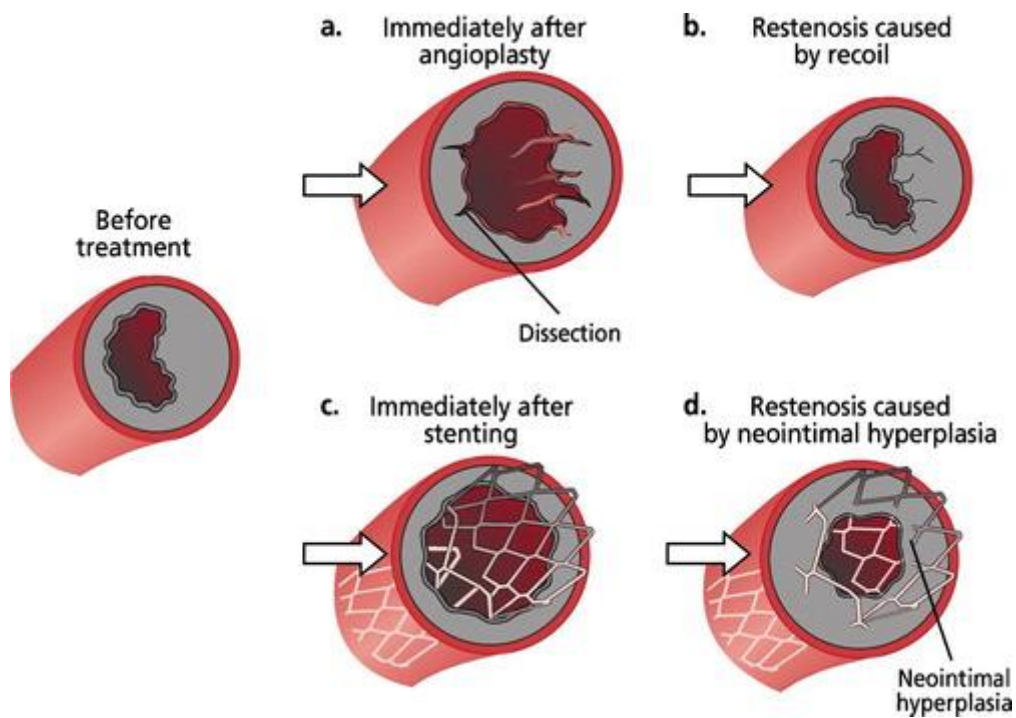


Figure 3. Restenosis of a coronary artery after balloon angioplasty(a-b) and after stenting(c-d) [19]

1.4. Aims

The objectives of this project were multifaceted and revolved around obtaining a more wholistic understanding of the materials and designs that are used in stents and how they contribute to modes of failure. Primarily, this study analysed simulations that were representative of stent performance and observed how various materials affected these values. Such values included stiffness in bending, linear compression, and radial compression as well as biocompatibility. Further, this project aimed to explore the interrelation between material and stent design to understand how such parameters could complement each other. This was devised to assist in designing better and more minimalistic stents that could work with alternate materials exhibiting favourable properties. The final aim was to suggest other materials that could be potentially used as stent materials and provide steadfast reasoning.

2. Chapter 2 – Literature Review



2.1. Evolution of Stents

Stents have gone through many evolutions in where newer materials and manufacturing methods have allowed for more complex stents to emerge with better performance. With these evolutions, superior designs are favoured over poor ones, with promising attributes being seen in later iterations. This section demonstrates the generations of stents with the corresponding highlights as well as downfalls.

Bare Metal Stents

The first generation of stents are known as bare metal stents (BMS) and were the first stents to be developed and given FDA approval. This includes stents such as the Palmaz-Schatz[®] (Johnson & Johnson) which was developed in 1987 and became the first stent to gain FDA approval[2]. This stent was comprised of stainless steel and was balloon expandable, seeing high usage throughout the 1990s even among other stents such as the Flexstent[®] (Cook) and the Wiktor[®](Medtronic). Although BMS stents reduced the percentage of cases having early elastic recoil and restenosis, there were still limitations. These stents had an increased risk of neointimal hyperplasia(NIH) which lead to cases of in-stent restenosis and stent thrombosis was an issue [5].

Drug Eluting Stents

The second generations of stents are drug eluting stents (DES). These stents are made from either metals or polymers and are generally coated by different drugs to provide different benefits. These stents initially consisted of mainly stainless-steel frames but have moved onto different alloys to allow for better mechanical properties including cobalt and platinum alloys [20]. DES were initially coated with antithrombotic coatings to solve the high restenosis rates in stents [21]. These worked and became commonplace due to their lower complication rates. Not all coatings could be planted on metal and as a result, some coatings require a polymer stent or a polymer stent with a metallic core to improve strength. Generally, DES do not perform as well as traditional bare metal stents due to the use of polymers and thinner struts being used. Currently, the drugs can have varying effects that range from

increasing biocompatibility through to reducing protein absorption and platelet adhesion, these can be found on vinylidene-fluoride which is a novel durable polymer coating [20].

There are two phases of DES, a first and second generation. The first generation occurred when it was determined that drug coatings could be administered with stents and were added on BMS with polymer coatings [22]. The second phase began when new materials were introduced, mainly being superior alloys such as cobalt chromium. Such materials offered better mechanical properties and allowed for the usage of thinner struts. The second generation of DES was intertwined with the emergence of bioresorbable stents which is depicted in Figure 4.

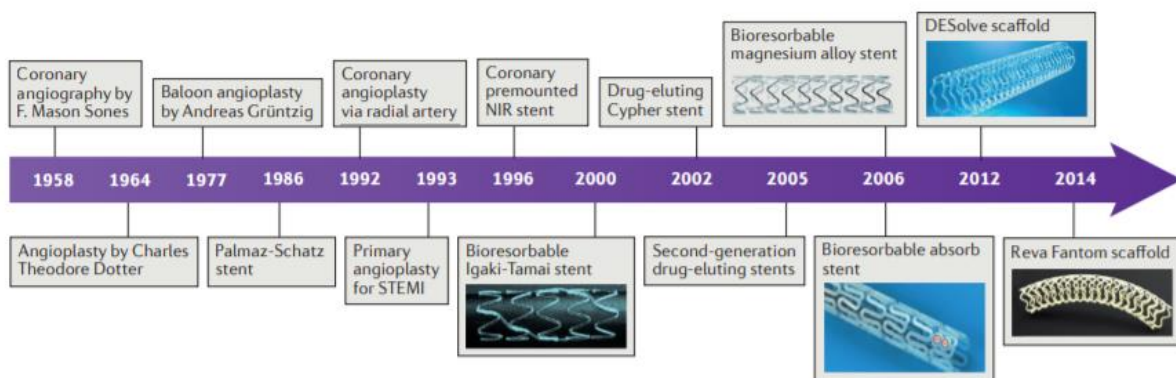


Figure 4. Milestones in Coronary Angioplasty [23]

Bioresorbable Stents

Third generational stents are known as biodegradable stents (BRS) as they slowly break down back into the body over time. Being part of the evolution of stents, these stents are aimed towards having the mechanical properties of BMS while also being able to be coated with drugs to reduce complications. From Figure 4 it can be noted at how recent bioresorbable stents have been prominent in the market. BRS are split into two divisions which are metallic and polymeric depending on what properties are desired. Figure 5 showcases the large variance in some properties between both bioresorbable metals, polymer based and BMS. One of the main problems currently with bioresorbable stents is that they do not perform as well as traditional stents. Lower elastic modulus and yield strength in these stents leads to larger struts to balance out the material's lack of mechanical strength. Figure 6 highlights just how large these differences in strut thickness can be. Such large struts lead to larger stents, being both less practical in delivery and flexibility while increasing the frequency of ISR.

Polymer composition	Tensile modulus of elasticity (Gpa)	Tensile strength (Mpa)	Elongation at break (%)	Degradation time (months)
Poly (L-lactide)	3.1–3.7	60–70	2–6	>24
Poly (DL-lactide)	3.1–3.7	45–55	2–6	12–6
Poly (glycolide)	6.5–7.0	90–110	1–2	6–12
50/50 DL-lactide/glycolide	3.4–3.8	40–50	1–4	1–2
82/18 L-lactide/glycolide	3.3–3.5	60–70	2–6	12–18
70/30 L-lactide/ ϵ -caprolactone	0.02–0.04	18–22	>100	12–24
Cobalt chromium	210–235	1,449	~40	Biostable
Stainless steel 316L	193	668	40+	Biostable
Nitinol	45	700–1,100	10–20	Biostable
Magnesium alloy	40–45	220–330	2–20	1–3

Gpa, Giga pascal; Mpa, Mega pascal.

Figure 5. Mechanical Properties and Degradation Time for Different Polymers and Metals [24]





Durable metallic stents			Biodegradable polymer-coated metallic stents				Bioresorbable non-metallic stents	
Xience/ Promus	Resolute	Onyx	BioMatrix	Ultimaster	Synergy	Orsiro	Absorb	DeSolve/Elixir
CoCr/ PtCr-EES	CoNi-ZES	PtIr-ZES	316L-BES	CoCr-SES	PtCr-EES	CoCr-SES	PLLA-EES	PLLA-NOV
								
81µm			Strut thickness					
91µm			120µm	80µm	74µm	60µm	157µm	165µm
Circumferential			Abluminal				Circumferential	
Polymer coating								

Figure 6. Comparison of the Strut Thickness of Different Categories of Stents [23]

2.2. Ideal Stent Properties

Due to how stents are deployed into their final position, they need to possess a range of specific properties to undergo the range of motions before they prop the vessel open. Properties such as high flexibility, low recoil and high yield strength if the stent is balloon expandable are needed for the stent to be delivered whilst once in place, high radial and tensile strength are required so the stent does not fail during operation [25]. Fatigue resistance is also highly sought after to increase the life span of the

stent. Other vital properties that enable the stent to perform properly include biocompatibility as well as the ability to be picked up in an x-ray or MRI. All these material characteristics can be broken down into three areas which is demonstrated in Figure 7 allowing for a simpler approach into these properties so that essential properties can be identified.

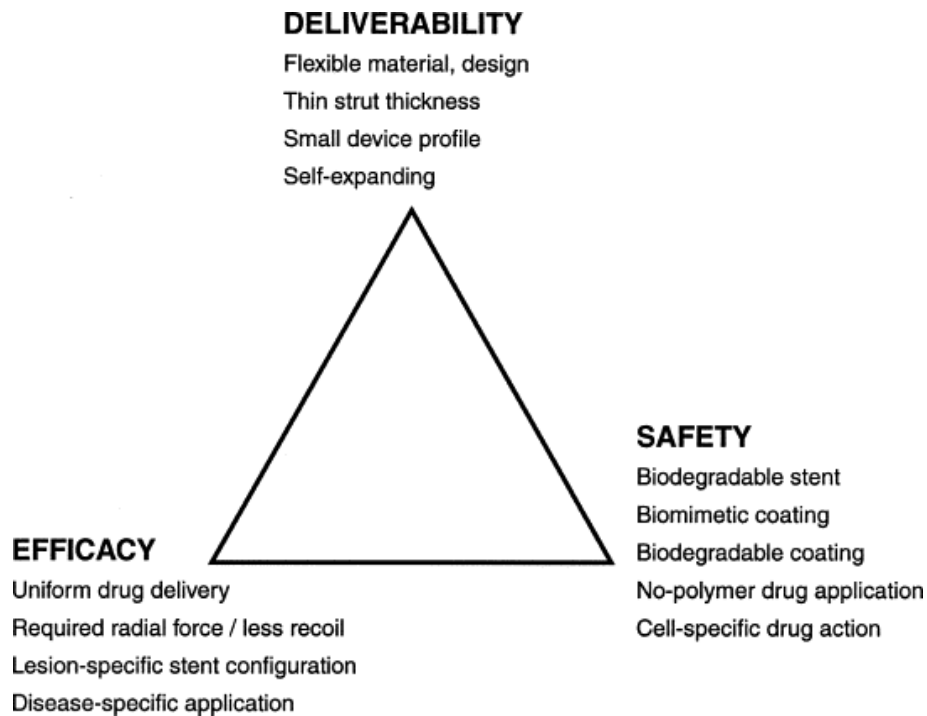


Figure 7. Design Criteria for the Ideal Drug-Eluting Stent Include a Multitude of Different, and Occasionally Conflicting, Properties, which may be Categorized from 3 Complementary Perspectives: Deliverability, Efficacy, and Safety. [26]

Deliverability

A requirement of stents is the ability to be moved through the body to the problem area where they can be deployed. This role is crucial as any premature failure will lead to problems over time. The characteristics looked at here are primarily stent flexibility, so that the stent can bend through blood vessels and not plastically deform before its intended destination [26]. Rogers et al. [27] describes that higher flexibility can be obtained through thinner struts, however this leads to less radiopacity. Model materials can allow for thinner struts but will maintain a radiopacity so they can be easily tracked. Hence, through aiming for thinner struts, materials with strong mechanical properties should be used.

Safety

Safety is a key property and must be a focus of the stent otherwise, additional issues may arise. Currently, the ways to implement this is through using biocompatible materials and having biomimetic coatings [27]. Another way to reduce vessel damage is to use biodegradable stent materials to reduce long term thrombosis. Advances in drug coating has enabled stents to possess properties including anti-proliferic and anti-inflammatory functions [27]. The material itself can also influence the safety of due to the release of metal ions over time which can lead to local inflammation. Palmaz et al. [28] determined that some metals such as 316L stainless steel and nitinol can corrode over time in the body leading to biotoxicity. Safety is of great importance in stent design which relies on many factors, mainly involving the stent material and coating which interact directly with the body and may give long term effects. Due to these safety factors, materials that have good mechanical properties should be checked for issues with safety.

Efficacy

Efforts to improve the efficacy of certain aspects of stents are currently where research lies. The desire to improve stent coatings so that negative effects are minimised is high. Ako et al. [26] demonstrates this through concluding that the ideal DES drug should inhibit proliferation while not impede the restoration of endothelial cells. Recoil is also an issue that is being investigated due to its efficacy. One study [29] determined that in certain self-expandable designs there could be a 23.6% increase in stent volume at a 6 month follow up when compared to its baseline and no such increase with a balloon expanded stent. Radial force is pivotal to this function and is required to hold open the vessel otherwise failure can occur. The efficacy of stents has been at the forefront of stent design and can improve both the safety and performance of stents, leading to lower rates of both short and long-term negative effects.

Hemodynamic Impact

The stent geometry is required to fulfil many objectives that will enable it to provide sufficient support and be safe at the same time, however, the geometry chosen will ultimately have an impact on the wall shear stress (WSS) of the blood vessel. Low WSS has been shown in studies [30] to lead to ISR and an abnormally high WSS that has been induced by a stent has a higher risk of stent thrombosis as well as

plaque rupture. To minimise the occurrence of such events, a study by Malek et al. [31] suggested that the wall shear stress should be below 0.4 Pa and above 1.5 Pa. Although the stent structure may not remove all shear stress outside this value range, they can attempt to minimise it to reduce the risks. The design of the stent can affect more than the structural performance of the stent but can adversely affect the surrounding tissue and alter the WSS to levels where there is an increased risk of damage.

2.3. Current Materials

This section outlines the current materials that are in use for stents today. Materials have been chosen to reflect all types of stents used in current industry. They have differing properties to demonstrate the variance and uniqueness of material characteristics.

Nitinol

Nitinol is a material comprised of nickel (Ni) and titanium (Ti), often in an equal ratio. Developed in the 1960's for the US navy, nitinol has become very prominent as a medical material due to its strength properties and biocompatibility. One of the unique features of this material is that it has a behaviour known as martensitic transformation which is more commonly known as super elasticity [32], allowing the material to return to its original shape when heat in the system is increased to a specified temperature. Additionally, it is non-corrosive and when used in a stent it is kink resistant, allowing it to be guided and placed easily with guidewires as described by Kapoor et al. [32]. One of the major drawbacks of nitinol has been due to its low density when compared to other metals, giving it low fluoroscopic visibility, which can be fixed by having other materials such as tantalum, integrated into the stent design itself [5, 32].

Stainless Steel 316L

Stainless steel has been a reliable material for stents and was the first material to be used for both BMS and DES[33]. It consists of mainly iron and carbon but also included other materials such as nickel(Ni), molybdenum(Mo), copper(Cu), titanium(Ti) and nitrogen(N) to increase properties such as corrosion resistance, heat resistance and strength [34]. The type of stainless steel that is most used in stents currently is 316L which includes molybdenum for corrosion resistance, increases the nickel and lowers

the carbon content in the structure. Although stainless steel 316L has been used for many stents and exhibits all round good properties, it does have drawbacks, mainly being pitting and crevice corrosion when implanted in the human body [34]. These localised spots of corrosion can contribute to the premature failure of the stent.

Cobalt Chromium

Cobalt-Chromium alloys can be very varied but for stent applications, Co-Cr L605 is commonly used. These alloys typically display stronger properties than stainless steel, including a higher elastic modulus and tensile strength which in turn allows for thinner struts. As this alloy has a higher density, the Co-Cr alloys demonstrate strong fluoroscopic visibility and a low ferromagnetic nature enabling it to be safe for MRI [5]. Much like stainless steel, it contains additional elements such as tungsten(W), nickel(Ni) and manganese(Mn) to produce better properties [35]. One of the main problems with this material is the potential for the localised release of cobalt and chromium ions from the stent, in turn causing inflammatory reactions [36].

Platinum Chromium

Flexibility is a key characteristic for stents currently which results in thinner struts, however this lowers the radiopacity of the device. Platinum chromium was designed to allow for thin struts whilst also being radiopaque due to the platinum. High corrosion resistance was achieved through the chromium which forms a chromium oxide layer [37]. Being a relatively new material that has not seen much use in stents, it could be a potentially high-performance material.

Magnesium Alloys

Magnesium has been viewed as an element that possesses a high biocompatibility, making it a forerunner as a stent material. Additionally, Chichareon et al. [5] noted that magnesium also has a high electronegativity which leads to an antithrombic effect which is highly favoured, especially in the design of stent scaffolds. Many stents use magnesium, a majority of these including the lekton magic coronary stent® [38] use a material known as WE43. This material consists of magnesium as well as yttrium and

zirconium in small amounts, less than 5%. Being a relatively new alloy, extensive testing has not been completed.

Zinc alloys with Magnesium and Aluminium

Being a relatively new material as a stent choice with limited testing, zinc provides both a high biodegradability and biocompatibility [39]. It is seen to be the middle ground between iron and magnesium and has reduced restenosis and improved procedural success according to Bowen et al. [40]. In a different paper, Bowen et al. [41] found in early testing that the corrosion of zinc is slow in the first three months and then increases afterwards. This has now been used with zinc magnesium alloys which offer a slower corrosion rate when compared to magnesium-based alloys enabling for the stent to hold open the vessel for a longer time. Zinc aluminium alloys were explored by Bowen et al. [41] and were found to have acceptable elongation and strength properties yet was determined to have higher early corrosion rates when compared to zinc. Zinc is a new material on the stent front and although it does not possess all the properties necessary for a stent material, when used in an alloy it can enable otherwise incompatible materials to be used.

Tantalum

Traditionally a material chosen for its anti-corrosion properties, tantalum has been used for stents but has never been used extensively. Boasting high mechanical performance and stability, Black et al. [42] determined that the reason of tantalum not being used is due to its fabrication issues. Mechanical issues were found when Jaschke et al. [43] tested the Strecker stent and discovered that 8 stents in a 30 patient sample had failure due to insufficient balloon dilation. Such failure was attributed to the rigid structure of the stent contributing to the low usage of this material. Tantalum is material that possesses strong attributes; however, production issues and rigidity have been problems in the past. With a re-design of the stent, a tantalum-based scaffold could allow for resilient properties and high performance.

Platinum Iridium

One of the main attributes of a platinum iridium alloy is its radiopacity, meaning it can be easily imaged. This alloy generally has a breakdown of 90% Pt -10% Ir and demonstrated high corrosion resistance

but Mani et al. [44] explained how the limited use of this alloy is due to a lack of mechanical properties. Testing demonstrated that it was safe to use in humans and that this alloy led to a lower rate of thrombosis and inflammatory reaction. However, the lacking mechanical properties will cause the stent to have much thicker struts to compete with other stronger alloys, being a problem.

2.4. Finite Element Analysis

Finite element analysis (FEA) is currently an accepted way of testing how devices and prototypes perform in the real world without physically crafting it. Through modelling, problems can be identified much earlier, and designs can be altered and retested in much shorter times than producing a new prototype. For these reasons, FEA simulations are common with stent design and multiple types of testing can be performed with high degrees of accuracy.

Axial Expansion and Compression

Axial loads are commonly experienced by stents and as such are often simulated in finite element analysis. Although generally it is expanded or compressed to yield, Mcgrath et al. [45] created a small asymmetry in one of the struts to create a forced buckling so that it could be observed and better tested. Chua et al. [46] graphed the change in the length of the stent and the effective diameter, demonstrating that these rates of change are not equal or linear. In such experimentation, there are secondary effects that can be measured and will affect the performance.

Radial Compression and Testing

Performance of a stent is indicated through numerous parameters including the ability to both repel and expand in the radial direction. As stents are required to hold the artery open, it is vital that they are proficient in this regard. It has been noted that this type of testing is more exhaustive when using different diameters to mimic variability in patients [47]. This paper has also put forward that when doing this testing in the radial direction, it is necessary to trace the strain and total artificial strain so that the artificial energy is negligible. From Figure 8, the radial compression test does not yield linear results and as such cannot be easily predicted, hence simulations should be conducted for this to reduce assumption errors.

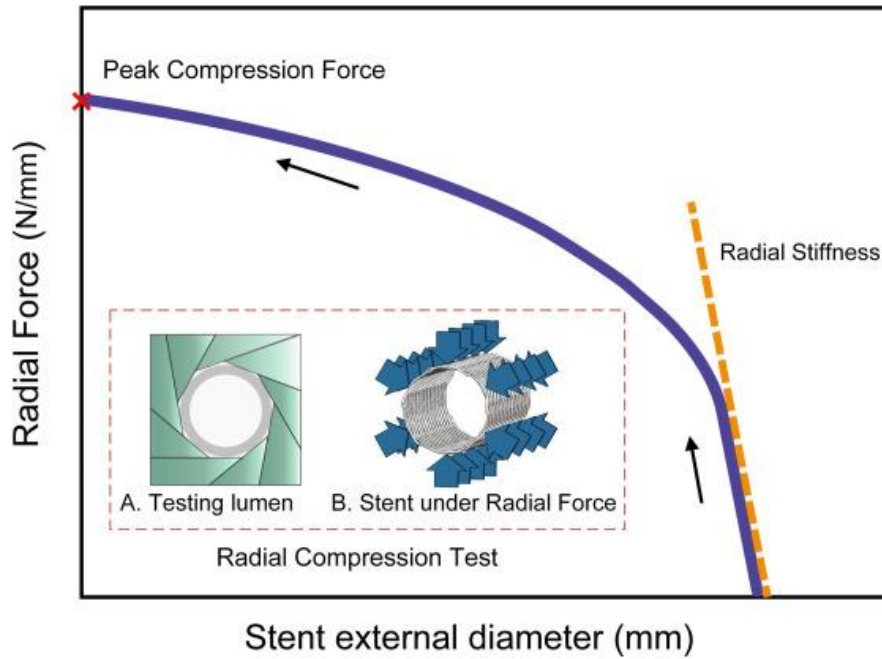


Figure 8. A Typical Radial Compression Curve of PLLA Braided Stent and Radial Compression Test.

Bending Test

Flexibility is a key component of a stent and is a requirement for its deployment. For the FEA simulations to be as accurate as possible, the material properties must be established for each tested material. Wu et al. [48] detailed how four point bending should be favoured over three point bending as it provides more accurate results due to it mimicking more realistic conditions. Additionally, it was pointed out that 3D simulations of bending allowed for more realistic results than 2D.

Fatigue Test

The longevity of a stent can be modelled through fatigue simulations to predict when cracking and mechanical failure will occur. Karanasiou et al. [49] described how the FDA requirements must be able to survive for 10 years or 10^8 loading cycles and that often, studies only require pulsatile flow when fatigue loading as this is what is anticipated from the heart. This was compared to Everett et al. [50] who used combined fatigue loading in bending, torsion and compression to create a more accurate fatigue loading simulations. Hence, to create more accurate simulations, multimodal fatigue loading should be used as opposed to a purely axial based pulsatile loading.

Material Properties

Material selection is based upon many factors ranging from mechanical properties to degradation rates and radiopacity. For FEA testing, mechanical properties will be required for each of the main materials that are currently used in market. These properties will enable for an accurate simulation of scenarios and can be found in Table 1.

Table 1. Material Properties of Current Stent Materials

Material	Density(g/cm ³)	Youngs Modulus (GPa)	Ultimate Tensile Strength (MPa)	Yield Strength (MPa)	Poisson's Ratio	References
Nitinol	6.45	83	1100-1200	560	0.3	[5] [51]
Stainless Steel 316L	7.95	193	668	366	0.265	[5] [52]
Co-Cr (L-605)	9.1	243	1147	629	0.29	[5] [53]
Platinum chromium	9.9	203	834	480	0.285	[5] [54]
Magnesium (WE43)	1.8	44.2	250	162	0.27	[55-57]
Zinc (magnesium)	1.8	44.8	380	275	0.35	[58]
Zinc (aluminium)	5	77.9	400-441	372	0.32	[59]
Tantalum	16.65	186	207	138	0.35	[5] [60]
Platinum Iridium	21.56	150	340	200	0.38	[5] [61]

Table 2. Material and Alloy Compositions

Material	Composition (%)	References
Nitinol	Ni 55, Ti 45	[5]
Stainless Steel 316L	Cr 17-19, Fe 60.5-67.75, Mn <=2.0, Mo 2.25- 3.5, Ni 13-15	[62]
Co-Cr (L-605)	Co 46.38 – 56.95, Cr 19-21, W 14-16, Ni 9-11, Fe <= 3	[53]
Platinum chromium	Fe 37, Pt 33, Cr 18, Ni 9, Mo 3, Mn Trace	[63]
Magnesium (WE43)	Mg 92, Li 0.2, Cu 0.3, Mn 0.15, Nd 2.4-4.4, Ni 0.005, Si 0.01, Y 3.7-4.3, Zn <= 0.2, Zr 0.4 - 1	[57]

Zinc (Magnesium)	Zn 91, Al 7.8-9.2, Zn 0.2 – 0.8, Mn 0.12, Si 0.1, Cu 0.05, Fe 0.005, Ni 0.0050	[58]
Zinc (Aluminium)	Zn 69.387, Al 28, Cu 2.5, Fe 0.075, Mn 0.02, Pb 0.006, Cd 0.006, Sn 0.006	[59]
Tantalum	Ta 100	[60]
Platinum Iridium	Pt 90, Ir 10	[61]

2.5. Experimental Testing

Computational models can yield accurate and realistic results, however, testing the real stents will allow for a benchmark and determine how accurate the computational models are. There are considerations that need to be examined with testing using the equipment and manufacturing methods available. Additionally, caution needs to be taken into account when keeping all factors the same, including maintaining the temperature in the testing room throughout testing [64].

Axial Tension and Compression

Testing the stent under axial loads will result in non-linear results and should use same testing inputs as the simulations. Considerations such as restricting the supports to minimise radial and torsion deformations need to be considered so that all forces are from axial loading [64]. Further, the methods that are used to clamp the stent ends should ensure that no stress concentrations are placed on the stent.

Bending

Experimental bending tests assist in determining the flexibility of stents so they can sufficiently bend. Mori et al. [7] explained that to determine the flexibility, the stent should not be bent in the radial direction as it may alter the results and lead to inaccuracies. It was also determined that if the design had an altering link pattern, then load the beam with even links so it is symmetrical and uneven bending does not occur.

Fatigue

Experimental fatigue loading allows for fatigue testing with in vivo testing conditions. Pelton et al. [65] tested nitinol through pulsatile fatigue loading, purely in axial loading. It was determined that although this was an indicator for the life span of the stent until fracture occurred, a multi modal loading would be beneficial and provide for a more accurate analysis.

2.6. Computational Fluid Dynamics

To measure the effect of a stent design on the blood vessel and the respective WSS, computational fluid dynamics (CFD) is often performed due to issues with testing in vivo. CFD is an analysis of the flow fluids using numerical solution method, often using the Navier stokes equation to assist in determining the pressure and velocity throughout the system [66]. This study assumed incompressible Newtonian viscous fluid, with spatially periodic flow and fully laminar conditions as is normally assumed with stent CFD analysis.

Such tests for stents are aimed at minimising the Low and High WSS tend to focus on certain design parameters such as the intra-strut angle [30] to find an optimal value. Often. The time averaged wall shear stress (TAWSS) is computed instead of LWSS due to the inflow being a pulse or wave to mimic the blood flow from the heart. By taking the TAWSS, the overall value can be evaluated as opposed to only at the peak flow.

2.7. Motivation For Research

Stent design is often at the forefront of stent research, although it is often limited by the materials chosen. Through a review of materials, it seems that various older materials that had promising potential were plagued with production issues which may not be present now. Currently, there is a shift towards bioresorbable metals and polymers with the metals not always performing adequately and dissolving too rapidly. Polymers lack the mechanical properties, with both having larger stent diameters to compensate, leading to flexibility issues. Second generation DES are believed to still have optimal performance over other generations of stents and as there are less papers testing this currently, there is a need to examine the current front running materials for their suitability.

3. Methodology

3.1. Overview

The primary aim of the thesis was to analyse and gain a deep understanding of how different materials used in commercial stent production affects their performance and relate this to their differing properties. This deepened knowledge would provide a framework to make more informed decisions when designing and developing stents in the future. This section intends to outline and explain how the various phases of the project were set up and executed to such an extent that one could replicate the computational simulations undertaken, and meaningfully understand the results. The breakdown and analysis on this data will be explored in chapter 5. In this thesis, the methodology was twofold, the first being to undertake analysis on stents within previous research, allowing for a comprehensive framework on material impact on various stent designs. This was executed using ANSYS 2021 and Katana on Demand, using the UNSW shared computational cluster. The second phase was to use the multi-objective optimisation process to create new stent designs with the previous materials listed as choices, building upon previous work to develop more advanced models and was completed through ANSYS 2019. Such a process was geared towards developing new stent designs with more variable material parameters, allowing the process to evolve over time.

In total, approximately 1000 simulations have been completed with the FEA testing 3 forces over 9 materials and 34 previously generated stents, this was increased with the created stents that required both FEA and CFD simulations to be ran. By the completion of the project, over 250 hours of simulations have been undertaken to complete all required work.

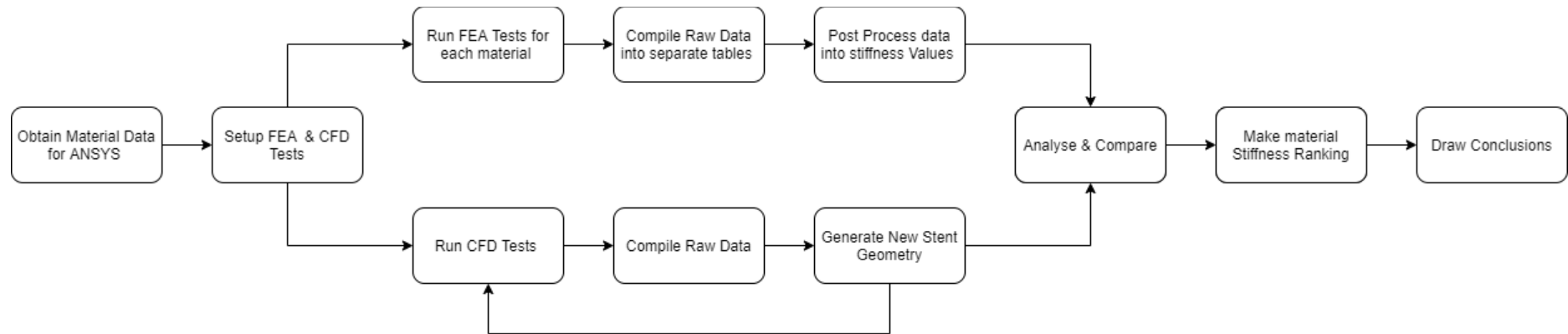


Figure 9. Flow Chart for Methodology

3.2. Stent Geometry

The stent geometry was developed using Iron python script, which is python script that is able to work on ANSYS software. The 34 stents used in the initial part of the thesis were based on previous work while the multi objective optimisation process formed new stent geometries to fulfil the objectives. The stent geometry script was developed to incorporate all design parameters of a stent, except for the overall diameter to allow for easy comparison and simulation set ups. The new stents that were to be generated would incorporate the type (Rectangular or Circular), SD1(Stent Diameter), SD2, SA(Strut Alignment), CH(Cell Height), AT(Alignment), CT(Connector type), NC(Number of Connectors) and the material. Table 3 details the various values that each of these parameters can undertake. For connector type, these were straight, spline and 'S' shape which were 1,2,3 respectively. The number of connectors denoted either 1, 2 or a 1,2,1 arrangement in numerical order. These changing parameters were used for all created stents. To assist in the visualisation of these various parameters, Figure 10 has been provided.

Table 3. Stent Parameter Values

Parameter	Type	SD1	SD2	SA	AT	CH	CT	NC	Material
Values	C or R	-	-	-	0,180	-	1-3	1-3	1-9

In the table above, the values that are discrete are shown with their range or options while values that are not are not displayed with a value. Alignment is 0 or 180 degrees and for the material options, the values 1-9 are given to the alloys that can be found in Table 1 in the order seen. For the circular type, a second stent diameter is not required as the first stent diameter will be the diameter of the strut.

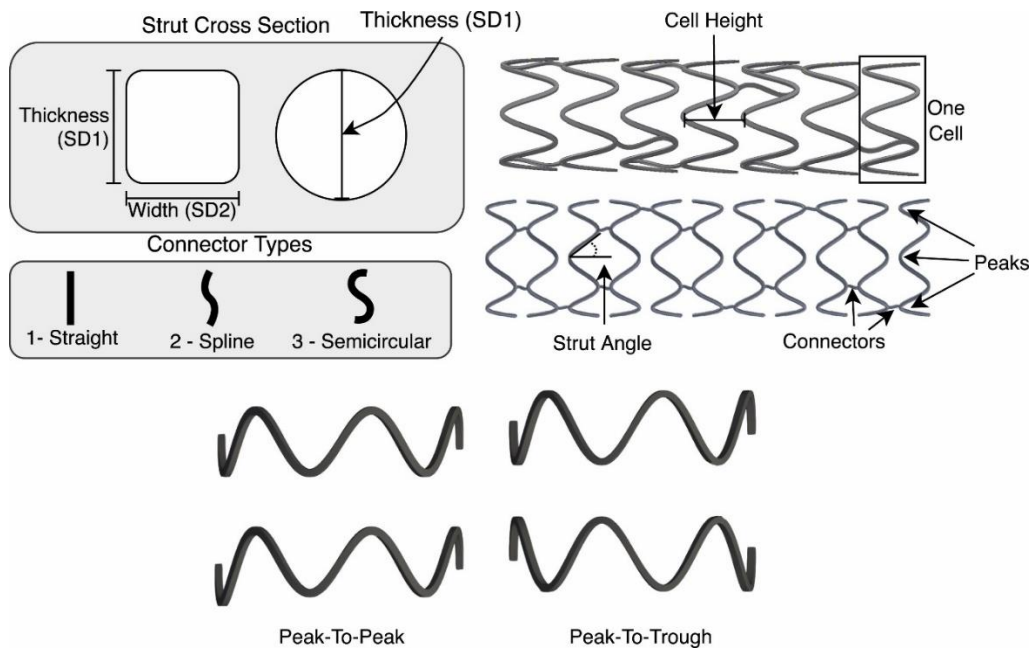


Figure 10. Stent Terminology and Design Variables [67]

3.3. Materials

The materials that were chosen to be included were Nitinol, Stainless Steel 316L, Cobalt Chromium, Platinum Chromium, Magnesium (WE43), Zinc Magnesium, Zinc Aluminium, Tantalum and Platinum Iridium. These materials are not built-in defaults in the ANSYS 2021 engineering materials tab and were input manually into the system before the execution of the simulations. This tab is found in the engineering data component of the analysis system and the location of the tab in the data page is shown in Figure 11. The addition of these materials was completed through opening the engineering data sources tab and choosing to create a new engineering materials folder. After this, each material is manually input with the key properties that are required to investigate (these are shown within Table 4 with the actual values for each material found in Table 1. These material values were implemented into ANSYS 2021 where a folder was created and could be used in any simulations.

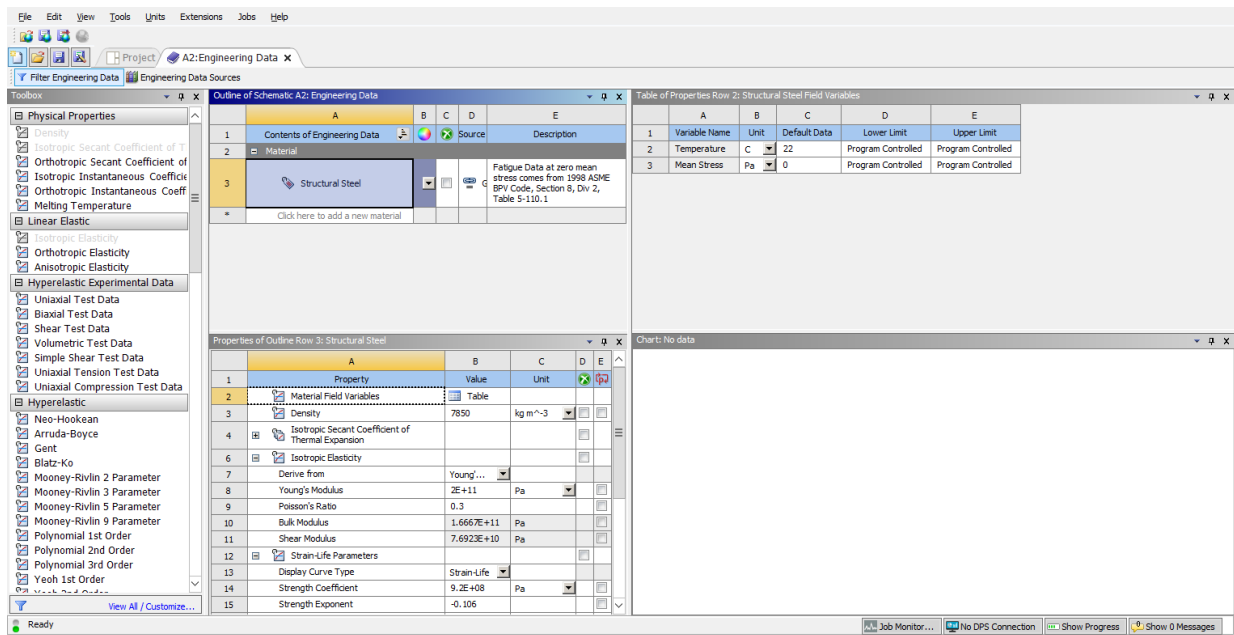


Figure 11. ANSYS 2021 Engineering Data Page

Table 4. Property inputs in ANSYS 2019 with units

Property	Units
Density	Kgm ²
Young's Modulus	GPa
Poisson's Ratio	-
Compressive Yield Strength	MPa

3.4. Mechanical Testing

The computational testing was undertaken using ANSYS 2021 on Katana on Demand, the UNSW HPC cluster. This allowed for higher performance when not at university so that simulations could be completed within a reasonable amount of time. For this part of the methodology, a base file was established that consisted of all the simulations to be run (compression, three-point bending and radial compression). These tests used the static structural module to assist in simulating real world conditions. Such simulations were designed to be in the elastic region of the structure to provide accurate simulation data for the anticipated loads of a stent.

The process itself involved importing generated stents into a base file which were then altered to fit the stent which included re-aligning the cylinder for compression and re allocating the location of the forces for the tests. Simulations were run as parameter sets so that larger quantities of simulations could be

run in series without manual reloading due to the large amount required to be tested. Table 5 demonstrates the force inputs for the various tests.

Table 5. Input Values for FEA Simulations

	Compression	Three-Point Bending	Radial Compression
Force (N)	0.004 N	0.01 N	0.02 MPa
	0.002 N	0.005 N	0.01 MPa
	0.001 N	0.001 N	0.005 MPa

The results of these simulations were moved into an excel sheet to keep record of the outcomes for all 34 stents, with each material having its own respective sheet. This was done as a simple and effective way to split data so it could then be conveniently manipulated and interpreted.

3.4.1. Compression

Compression simulations were designed to reflect the compressive forces often incurred by stents during and after deployment. The simulations for the compressive strength of the stent involved keeping one end of the stent as a static support and applying an inward force on opposite ring. This simulation has been validated through previous students work, V. Luvio [68] and A. Senthumathan [69] who originally based it off Ormiston et al. The forces that were applied in the compression simulation are highlighted in Table 5 to establish the compression over a wide range of forces.

Figure 12 provides visual representation of how the simulation looked when being set up, representing the fixed support located at ring B and the force applied in the Z direction from ring A to compress the stent. The force and fixed support are at the ends of the stent irrelevant of length as that will be factored in during a later phase.

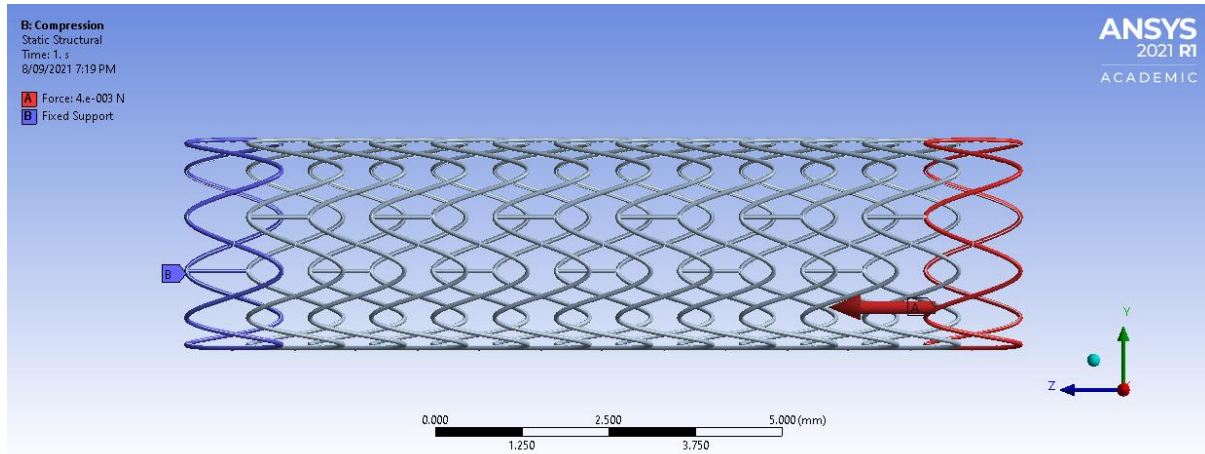


Figure 12. Ansys 2021 Compression Simulation

The output properties of this simulation will revolve around the various stresses and strains encountered by the body as the force changes. These outputs that will be calculated by ANSYS are expressed in Table 6.

Table 6. Outputs for Compression Simulation

Output	Directional Deformation Ave	Directional Deformation Max	Directional Deformation Min	Equivalent Stress Ave	Equivalent Stress Max	Equivalent Stress Min
Unit	m	m	m	Pa	Pa	Pa

Processing this raw data will enable for comparison between stents due to their differing lengths and structures. For the longitudinal compression simulations, the data will be converted to compressional stiffness. This will effectively find the spring constant as if we were using Hooke's Law.

This is expressed within equation (1) , where k is the compressional stiffness of the stent in N/mm, F is the force applied in N and x is the measured deformation of the system in mm. From the raw data, the force applied on the displaced end and the directional deformation maximum is the input. Maximising the compressional stiffness will provide an optimal strength of the stent to resist the longitudinal forces and minimise stent recoil in that direction.

$$k = \frac{F}{x} \quad (1)$$

3.4.2. Bending

The three-point bending simulation was designed to mimic conditions that are anticipated for a stent when being implanted and during use. These forces could come due to the movement of a blood vessel or when the stent is being implanted into the body. Although previous work calculated that four-point bending would improve accuracy, this was not possible due to technical difficulties in applying an even force due to the lengths between these applied forces and the rings. As the simulations were kept as three point-bending these could be completed using methods from previous work. Primarily, this method revolved around applying a singular force at the mid-point of the stent while the ends are restricted in movement through the implementation of cylindrical supports. This was chosen as the support point due to its simple way to create and to help avoid a singularity.

The stent cylindrical supports were placed on both sides of the stent with the difference between being the active length, which is the length between the midpoint of the first ring and the last ring. In generating the cylindrical supports, the radius and thickness are up to the experimenter's discretion to choose such that they will not affect the simulation, nor be an infinitesimally small region. For the simulations, the locations of the cylinders were automated using the parameter function of ANSYS. This function used the active length to accurately place the cylindrical supports. The applied force was added manually to a ring of the stent. This allowed for the middle ring to have the force applied, minimising stress localisations. The overall setup of the three-point bending simulation is demonstrated in Figure 13.

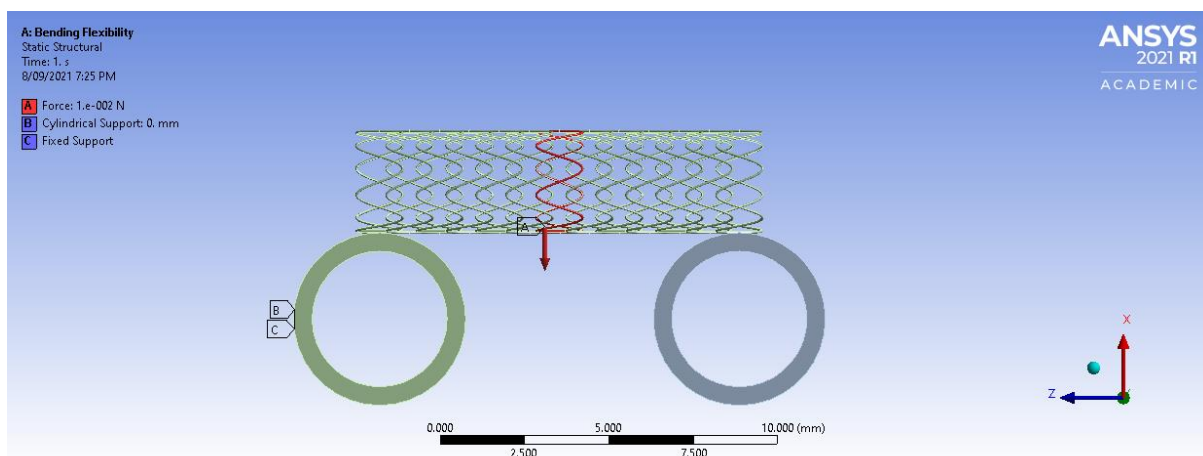


Figure 13. Three Point Bending Simulation

With the completed bending simulation setup, the input application of forces and the gathering of results began. The simulation forces are shown in Table 5 for this simulation. These forces were put in the design parameter and were converted into the measured outputs shown in Table 7. These output values serve to both provide raw data to be manipulated into meaningful results and to help assist that the simulations are working as anticipated.

Table 7. Output Values for Three-Point Bending

Output	Directional Deformation Ave	Directional Deformation Max	Directional; Deformation Min	Equivalent Stress Ave	Equivalent Stress Max	Equivalent Stress Min
Unit	m	m	m	Pa	Pa	Pa

Concluding with the collection of the results, the data was converted into values that can be compared, regardless of the variation of length or other variables. In the bending test, this value is the bending stiffness. This type of stiffness is the resistance of a certain member to bending deformation and a lower bending stiffness will benefit the stent in that it can be implanted with more ease and efficiency as well as reduce stress between the expanded stent and surrounding tissue [48]. The bending stiffness can be calculated by using equation (2), where EI is the bending stiffness in Nmm^2 of the structure, F is the normal force applied to the structure, l is the active length of the stent and δ is the maximum deflection of the structure.

$$EI = \frac{Fl^3}{48\delta} \quad (2)$$

3.4.3. Radial Compression

Radial compression is a vital simulation to complete when attempting to validate a novel stent design. Failure in this mode will result in a catastrophic failure, which is why such a robust simulation has been created. Formed by Kumar et al [70] and used by prior students [68, 69], this method involves generating a stent and using a cylinder at sliced intervals to apply the radial force, mimicking a blood vessel.

In design modeller, a part of the ANSYS software suite, the stent was imported via the external geometry attachment tool. Once the stent is imported, slices were created at the median ring locations,

in these simulations it was formed in the XY plane to slice through a single ring. After this was completed, a cylinder was formed to a chosen diameter so that it slightly overlapped on the outside of the stent, allowing for the force to be applied to just the outer layer as the overlap was where the force was applied. The stent and the cylinder parts are separately grouped into a stent and cylinder combination respectively. The figure that has been developed should look akin to Figure 14 and its respective layout.

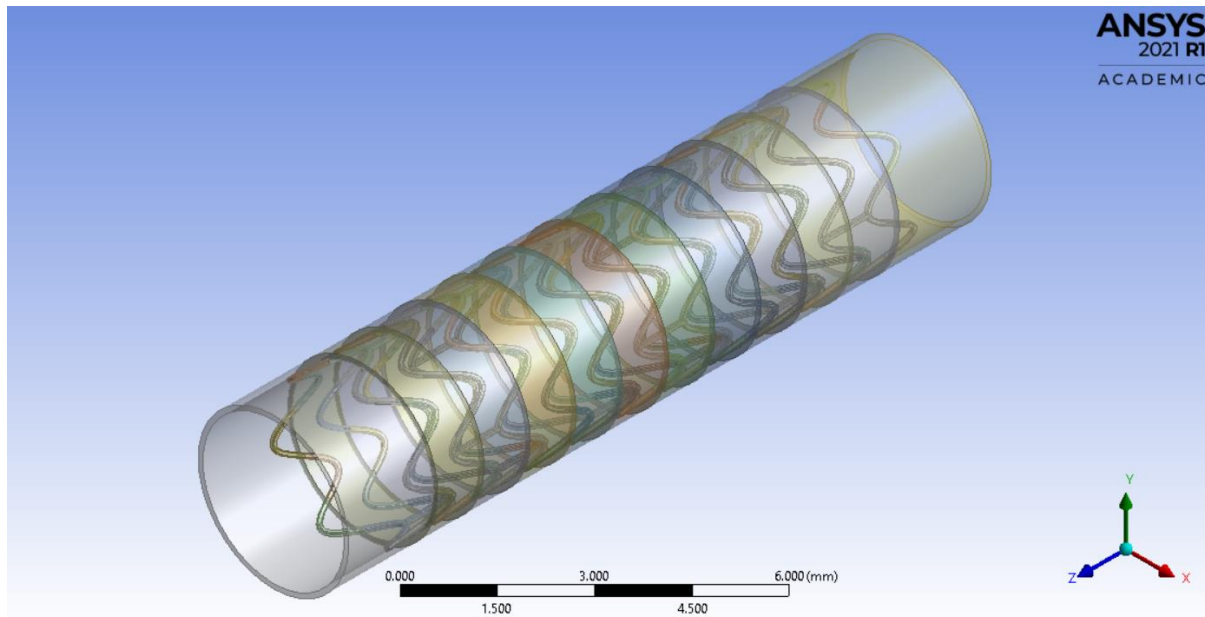


Figure 14. Radial Compression set-up in Design Modeller

Once this has been accomplished. The model is loaded in ANSYS static structural where the interface between the two objects is selected, i.e., the outermost section of the stent. This selection becomes the location for the pressure applied on the stent. This is to mimic the blood vessel's pressure squeezing the stent, which must resist deformation. The pressure will be applied towards the centre of the stent, and at this point, note the surface area of this force as a parameter as it is to be used in later analysis. The model set up is shown in Figure 15 and demonstrates how it should look like when formed. In this model, the pressure is applied to the outer surface and the deformation is calculated from the slices in the midpoint of the stent rings.

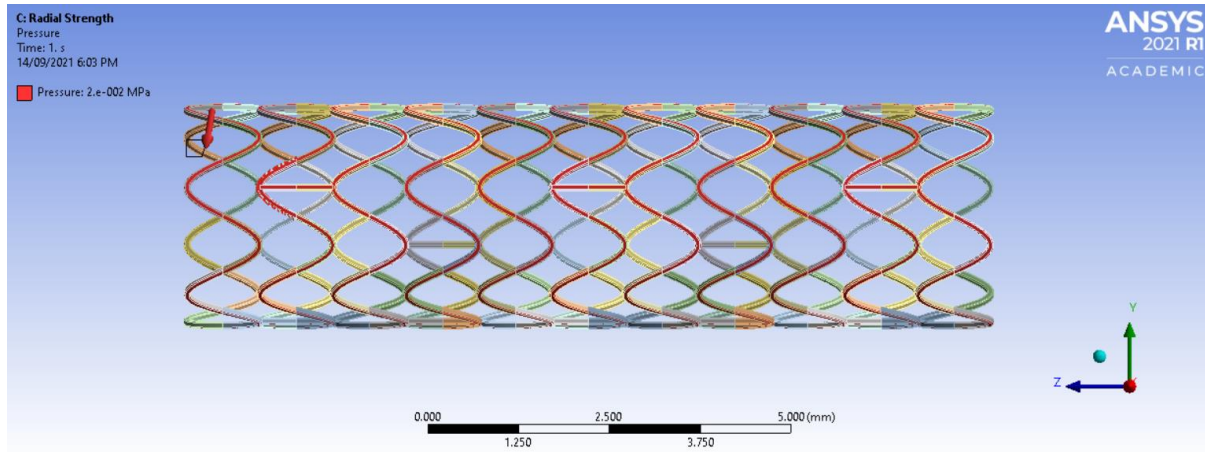


Figure 15. Radial Compression Model Set-Up

Once the setup has been completed, the outputs were again calculated through the parameter set function where the applied pressures are inputted. These input values are detailed in Table 5. The measured outputs of the simulation are outlined in Table 8, varying slightly from the previous simulations. These values are then converted into other forms, including radial stiffness. The radial stiffness is calculated to allow for comparison of the different stents due to the varying surface area. It can be calculated through using equation (5) which is constructed using equation (3) and equation (4). In these equations, D_1 is the original diameter while D_2 is the change after the force was applied or twice the deformation to account for both sides of the stent. Equation (4) calculated the force through the input pressure (P) and the surface area of the outside of the stent where the pressure was applied (A). Equation (5) combined the previous two equations in finding the stiffness in the radial direction through N/mm.

$$\Delta D = D_1 - D_2 = (3mm - 2 \times \delta) \quad (3)$$

$$F = P \times A \quad (4)$$

$$Radial\ Stiffness = \frac{F}{\Delta D} \quad (5)$$

Table 8. Outputs of the Radial Compression Simulation and respective Units

Output	Total Deformation	Total Deformation	Total Deformation	Equivalent Stress	Equivalent Stress	Equivalent Stress	SA
Unit	mm	mm	mm	mPa	mPa	mPa	mm ²

3.5. Multi- Objective Optimisation process

The multi-objective Optimisation process has been developed to propose new stent designs that would evolve over time to form stents with better performance characteristics than currently used models. To complete this task, both CFD and FEA analysis was required as well as the ability to generate stents.

To create new stents, a multi-objective optimisation code was developed on MATLAB to produce a new stent based on the results from previous trials. Here, the aims were to maximise radial compression, minimise Low Time averaged wall shear stress (LTAWSS) and high wall shear stress (HWSS). These objectives were to be optimised through changing the various parameters of the stent which were detailed in section 3.2. The MATLAB scripts inputted data from an excel sheet containing the parameters for a particular stent as well as their performance in certain objectives. These objectives were to be kept the same as prior students [68, 69] to provide an ease of use as well as for a streamlined comparison between students results.

The optimisation parameters in the multi-objective optimisation process were to minimise LTAWSS, minimise the HWSS and maximise the radial stiffness of the design. These objectives were chosen to be the most prominent and effective ways to improve stent design with the limitation of the code to optimise three objectives. The specific values of the CFD objectives are outlined in Table 9.

Table 9. CFD objective threshold values

CFD Value	TAWSS	HWSS
Range	$\leq 0.5 \text{ Pa}$	$\geq 3 \text{ Pa}$

The CFD values are generated through the CFD code that has been provided and tested through students in the past [68, 69].

The stent was carved into a tube with the Boolean subtract feature on ANSYS 2019. This base file was uploaded along with other code to provide a .txt file that contains all vital information pertaining to the multi objective optimisation process.

The results of the multi objective optimisation process are the objectives that are assessed throughout the process. As the optimisation evolves and develops, the objectives should slowly move towards more ideal and optimal values.

4. Results

This section details the results that were obtained during the execution of the project, with the methods outlined in Chapter 3. The results are split into two sections to reflect the two separate methods and hence, different post processing. The first segment explores the finite element analysis methodology, analysing this portion of the project and the data that has been obtained to explore the variance between materials. The second part highlights the multi objective optimisation process which revolves around generating new stents in the search of higher performance and lower impact.

4.1. Finite Element Analysis – Base Results

The FEA testing obtained results that depicted the stresses and deformation for each of the stents, these quantities were converted to stiffness values for each simulation to evaluate the stiffness of each material choice. This is plotted in Figure 16, Figure 17, Figure 18 respectively evaluating the compression, bending and radial stiffness for each type of simulation that was run. The complete set of data for all materials in these tests can be found in appendix

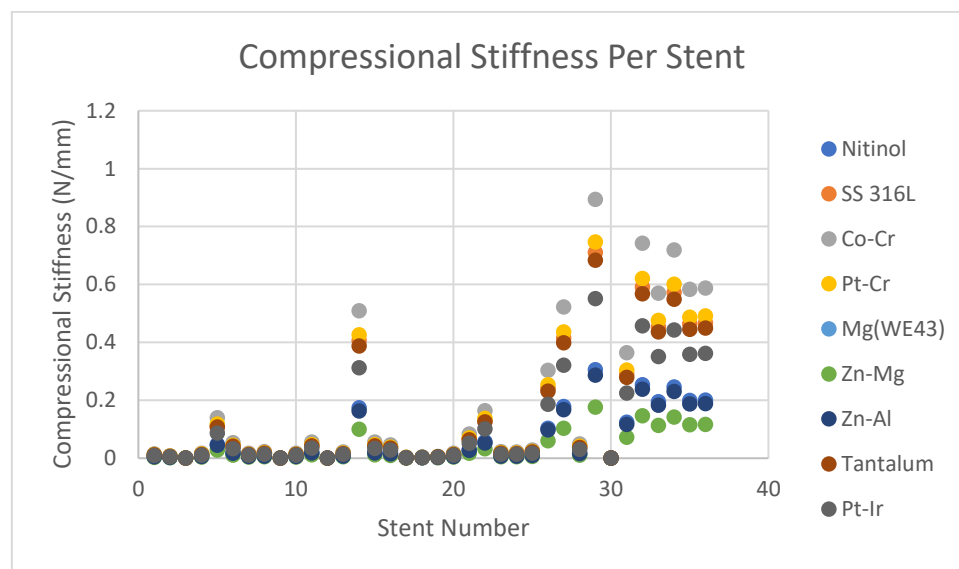


Figure 16. Compressional Stiffness for Stents

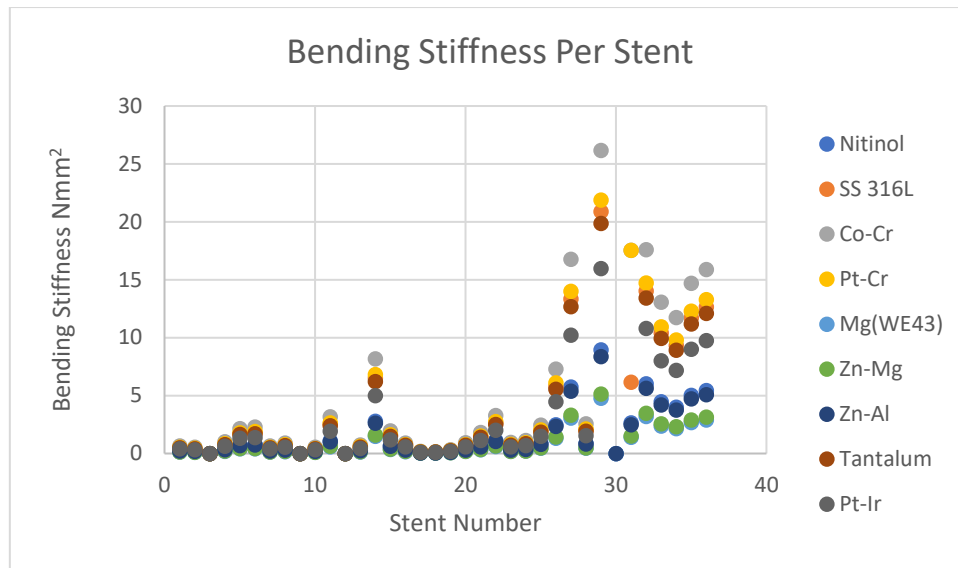


Figure 17. Bending Stiffness for Stents

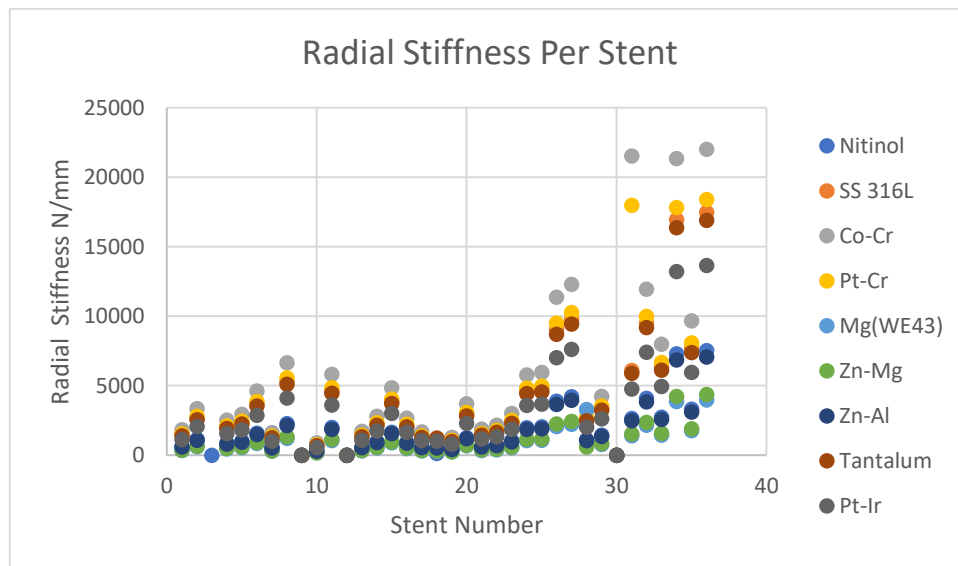


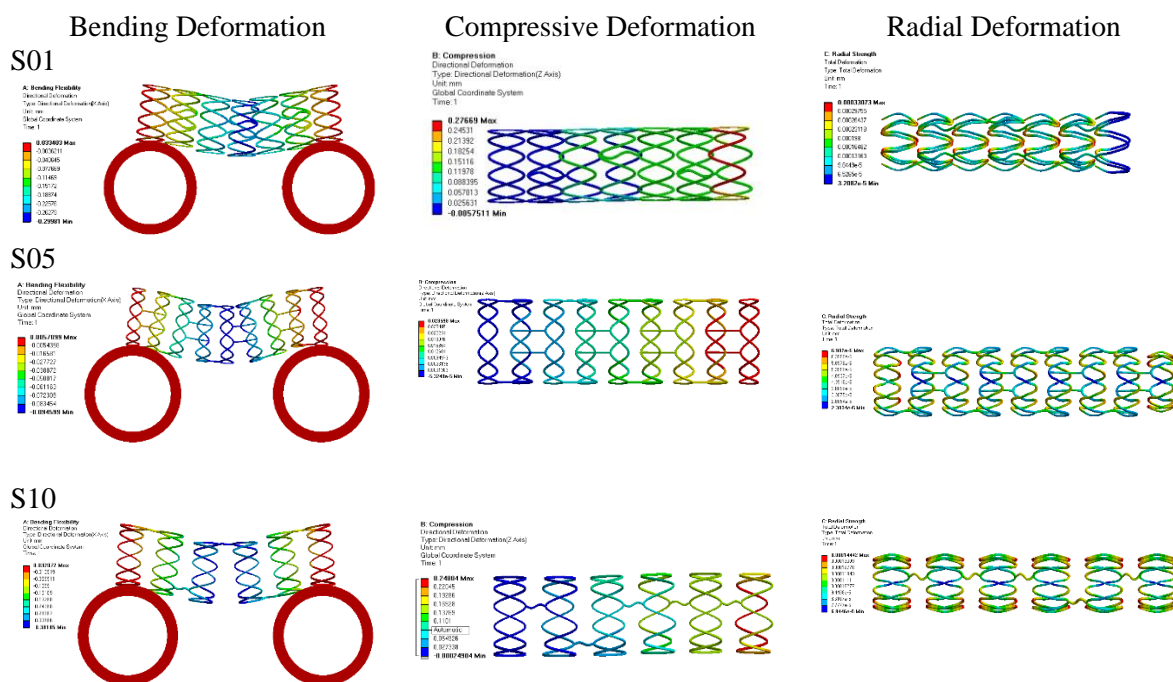
Figure 18. Radial Stiffness for Stents

Each of these graphs has produced the same stiffness ranking across the various simulations which has been tabulated into Table 10 for comparison. Multiple stents were used to create this stiffness graph to ensure that the rankings were purely indications of the material properties and not the stent design. The Stiffness value at the end shows how stiff the material is compared to cobalt chromium to help understand by how much a material is more pliable.

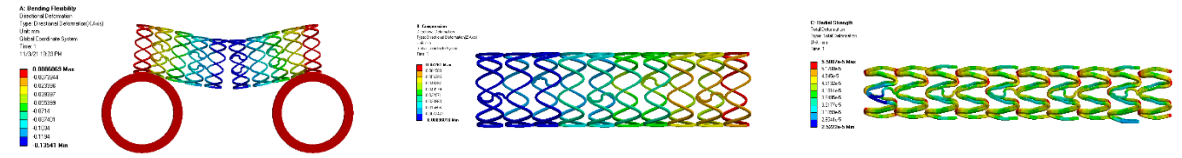
Table 10. Stiffness Ranking Table

Ranking	Material	Relative Stiffness Value
1	Cobalt Chromium	1
2	Platinum Chromium	0.836
3	Stainless Steel 316 L	0.796
4	Tantalum	0.761
5	Platinum Iridium	0.612
6	Nitinol	0.341
7	Zinc – Aluminium	0.320
8	Zinc – Magnesium	0.196
9	Magnesium (WE43)	0.181

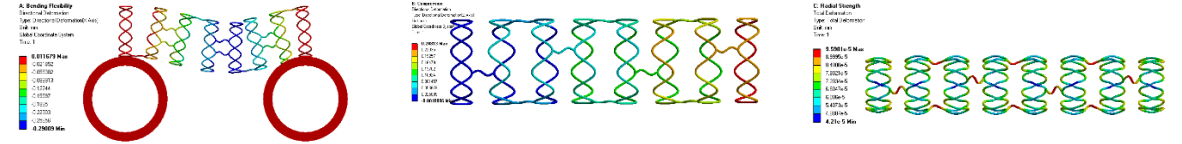
Simulations on ANSYS allowed for visual depictions of where the deformation and stresses are focused and how the stent will look after the force was applied. Images for these simulations were taken at 5 stent intervals when available due to not all stents having viable geometries to assist in demonstrating how the stents have changed in performance over time. Figure 19 explores the deformation of the stent in the three different loading types in which red is the maximum deformation and blue is the minimum deformation, except for three-point bending in which it is the opposite. Analysing the bending deformation, the maximum can be seen at the centre ring and the connectors, with the load being less prominent the closer to the support. In the compression simulations, the greatest deformation is found where the force is applied, especially on the side where there is no connector present. In the radial compression simulations, the maximum deformation is in the peaks of the rings whilst the centres resisted deformation better. Much like the compression simulations, there is less deformation where there is a connector as there is more material to take the load.



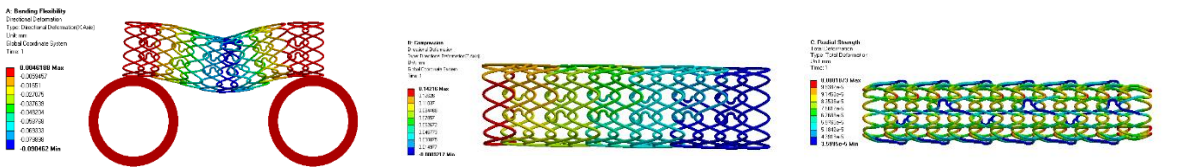
S15



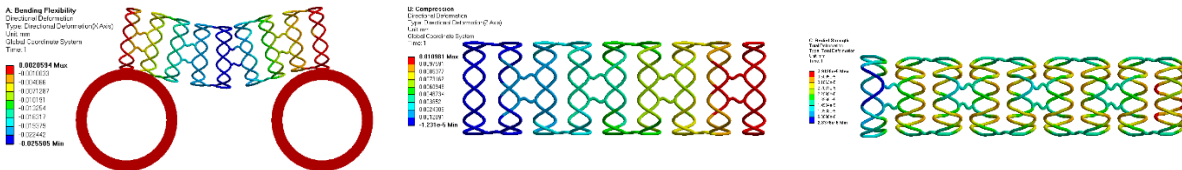
S20



S25



S31



S35

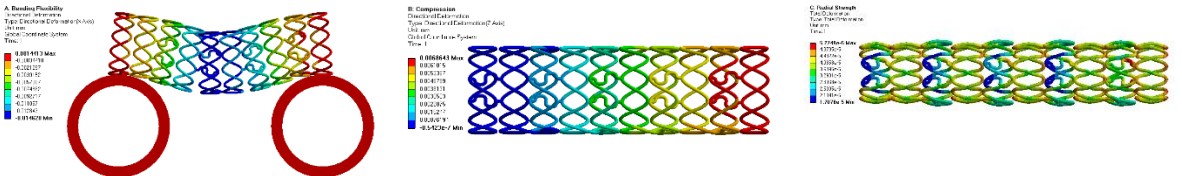
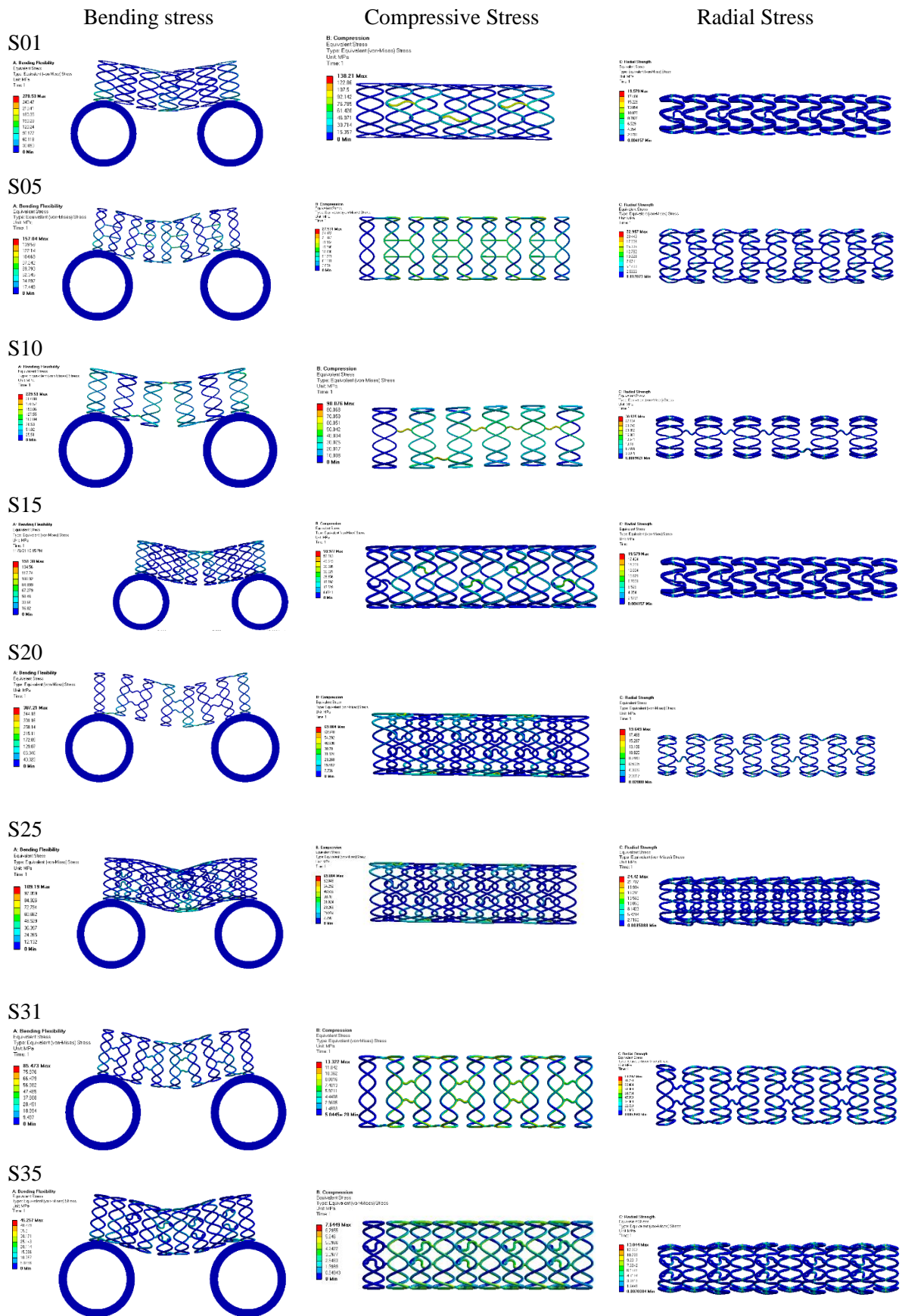


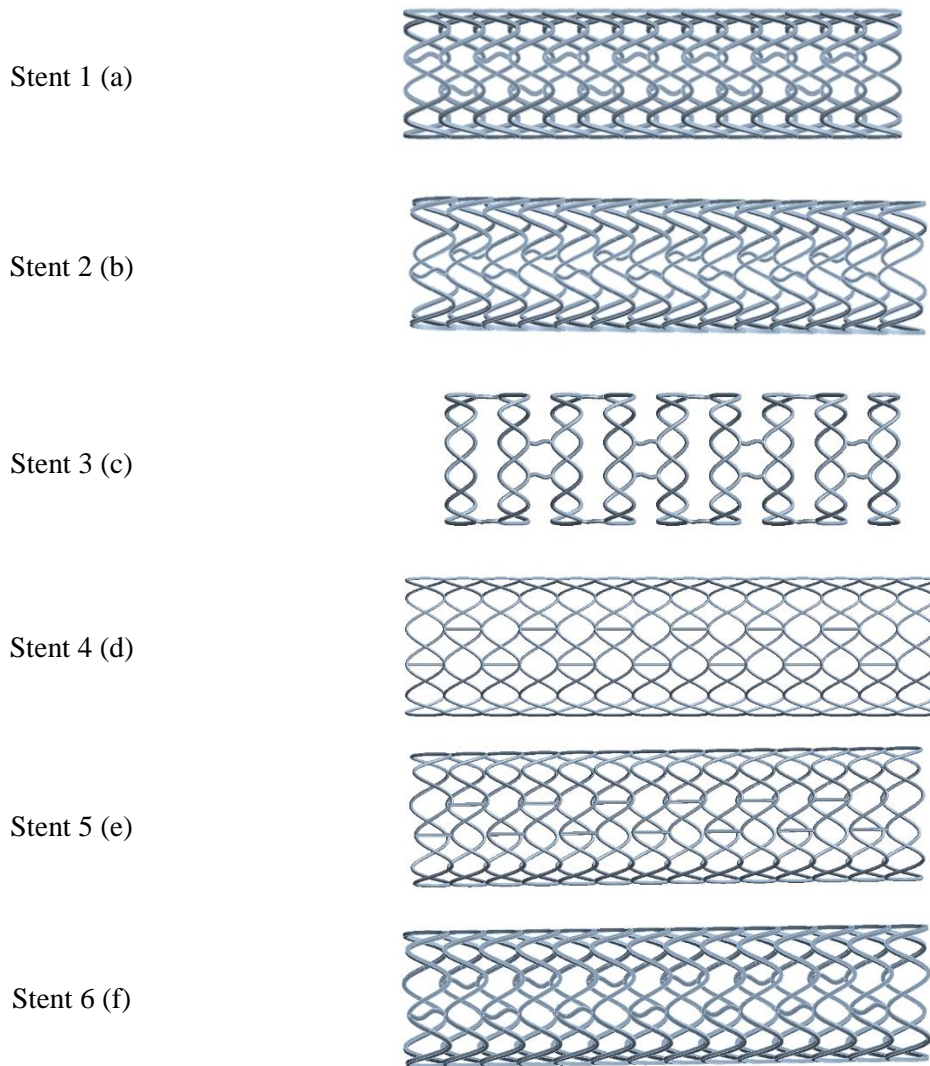
Figure 19. Simulation Deformation for Select Stents

Figure 20 conveys the stresses of the stents at regular 5 stent intervals when available as not all stents produced data to show where the stress concentrations are and to show how the optimisation code deals with such effects over time to minimise them. In these simulations the lowest stresses are in blue and work up until they are red for the maximum stresses. Bending simulations possess the maximum stress at the connector that undergoes the greatest bending forces. With the compression simulations, the majority of the stress is similarly concentrated in the connectors. Radial stress follows deformation with the concentration of load being in the centre of the cell and in the connectors.



4.2. Multi Objective Optimisation Process

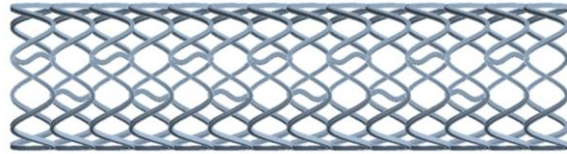
The multi objective optimisation process created 10 novel stents from the optimisation code where the created geometries can be found in Figure 21. This process evaluated the performance in both FEA and CFD, where the numerical values of such tests and initial parameter values are located in Table 11. The complete set of performance parameters can be found in Appendix C for a deeper insight into all performance characteristics, not only the code parameters. Figure 21 showcases the created geometries so it can be seen how these novel designs look as well as to show how these geometries are changed through each iteration.



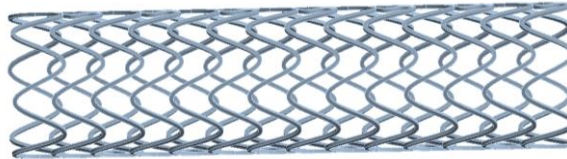
Stent 7 (g)



Stent 8 (h)



Stent 9 (i)



Stent 10 (j)

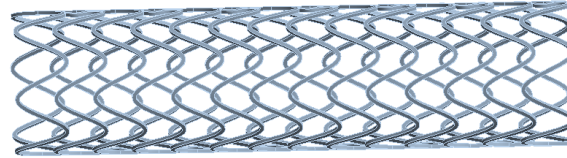


Figure 21. Multi Objective Optimisation created Geometries. (a.b.f.h.i,j) Rectangular type Stents. (c,d,e,g) Circular type Stents

Table 11. Created Stents Sample Performance and Parameter Values

STENT	Type	SD1	SD2	SA	Align	CH	NC	CT	Material	LTAWSS (%)	HWSS (%)	Radial Stiffness (N/mm)
1	1	91.108	93.1753	36.5385	0	0.83	1	2	8	22.75956	56.18036	3991.518
2	1	89.1406	74.9234	37.8802	0	0.83	1	2	8	22.1322	42.29394	2136.199
3	2	99.2308	Inf	49.003	180	0.83	2	2	6	10.61673	69.4029	1522.225
4	2	60	inf	43.0582	0	0.83	1	1	7	9.152891	69.58186	732.3869
5	2	79.2311	Inf	42.5704	0	0.83	1	1	7	12.41426	57.09939	1194.564
6	1	87.1513	90.6498	39.8737	0	0.83	1	2	8	21.4677	43.29903	3283.877
7	2	101.0533	Inf	47.8106	180	1	2	3	6	13.78006	65.70155	1594.28
8	1	101.7206	84.2069	41.8313	0	0.83	1	2	8	24.42313	40.60851	3687.697
9	1	77.921	84.4471	36.1248	0	0.83	1	2	8	20.43605	44.83751	2092.287
10	2	115.7914	Inf	33.5536	180	0.82	2	2	1	20.83358	45.86863	9792.468

The multi objective optimisation code generated new stents and also produced a three-dimensional graph that showcased how the three objectives were fulfilled through stent iterations. All stent geometries were plotted and broken into circular and rectangular stent types as well as the most recent selection to provide a breakdown in performance based on these parameters.

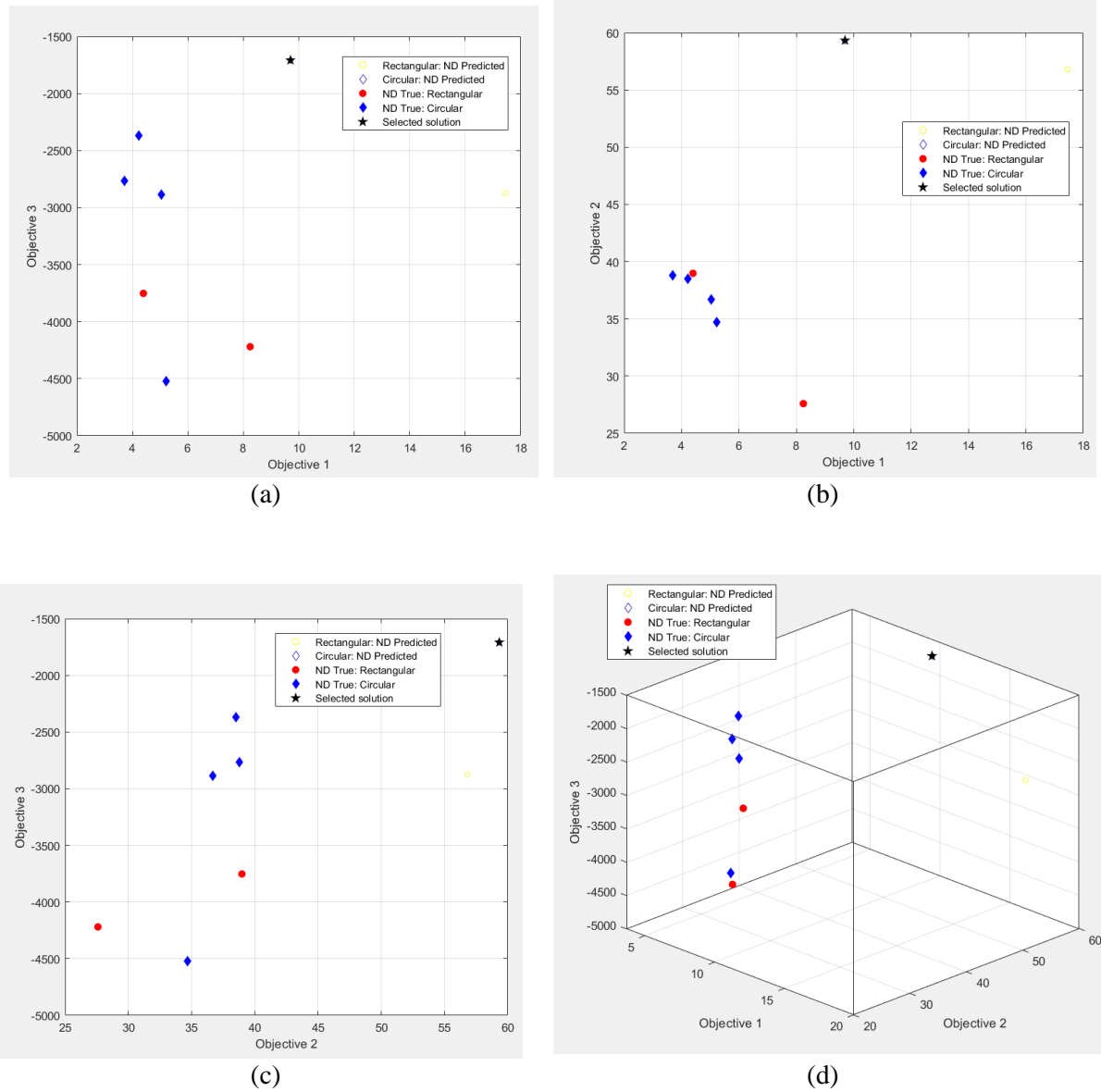
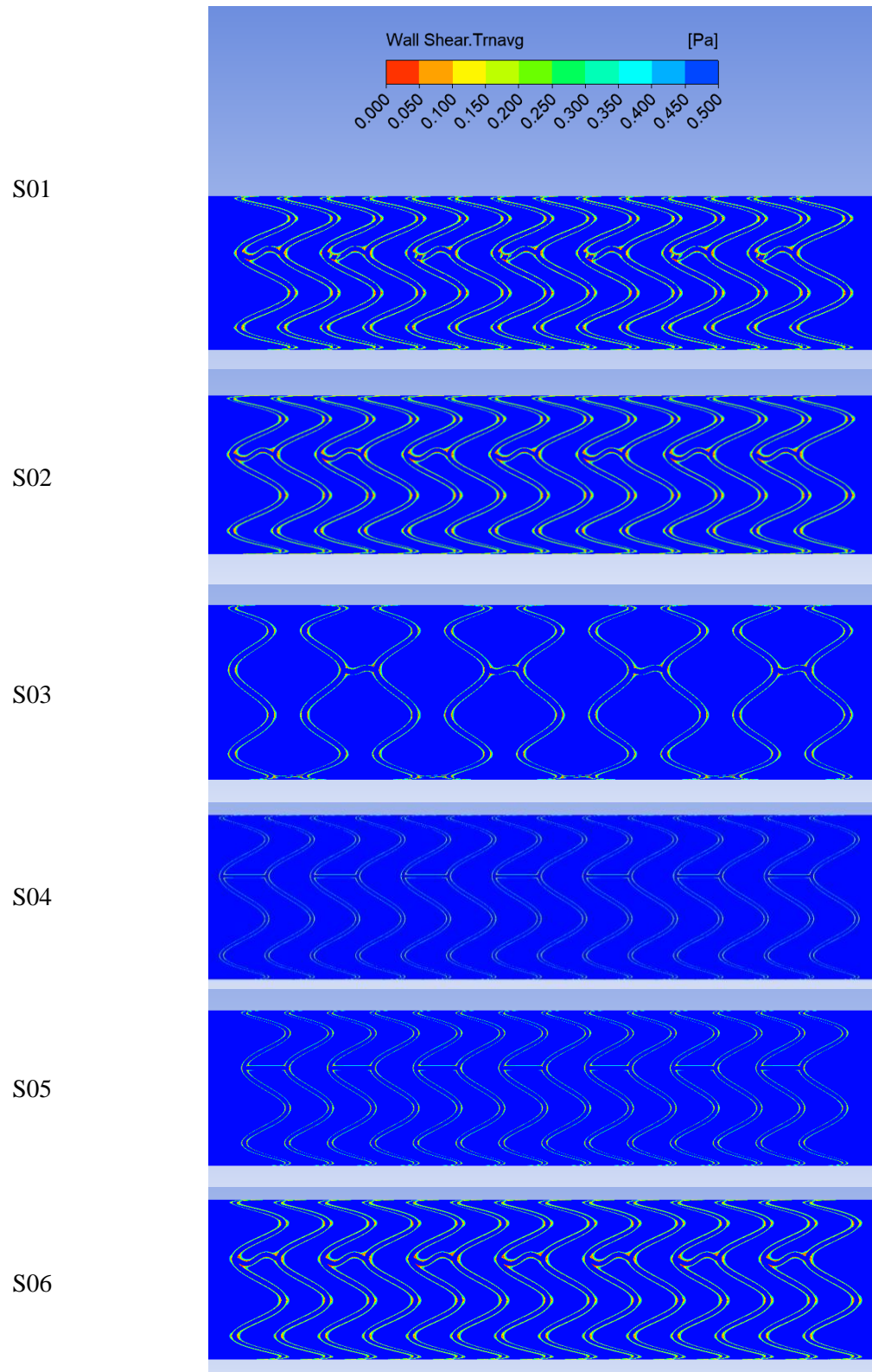
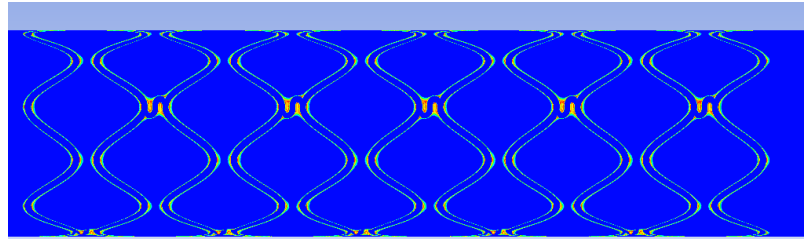


Figure 22. Performance Graph of Created Stent geometries, (a) compares LTAWSS and radial stiffness, (b) compares LTAWSS and HWSS, (c) compares HWSS and radial stiffness, (d) compares all three parameters

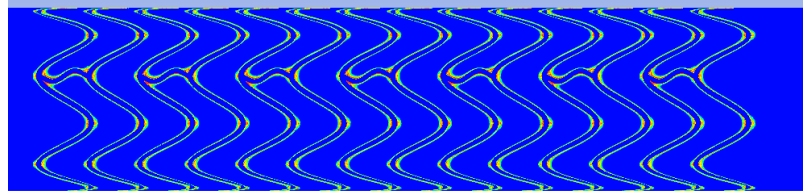
Figure 23 denotes the LTAWSS distribution along the stent for the created geometries using the optimisation code. It can be noted that parts where abnormally low shear stress occurs is near the stent geometry, especially at the joint between the connector and the ring.



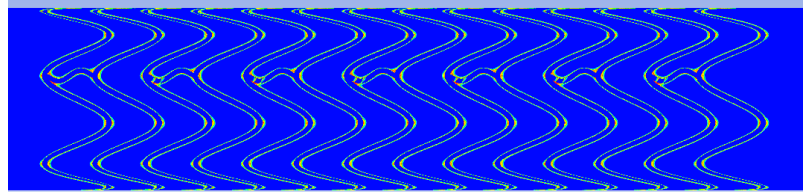
S07



S08



S09



S10

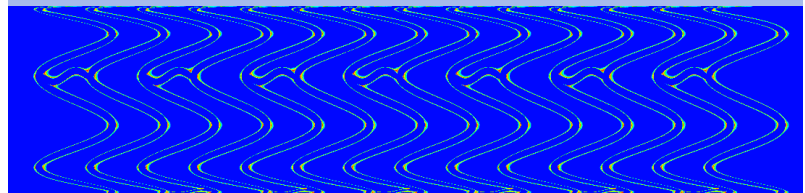


Figure 23. LTAWSS for Created Stents. Low wall shear stress as a time average in the given flow rate and same vessel geometry

5. Discussion

The project successfully addressed the desired aims through the simulations conducted and provided additional insight into multiple aspects that play pivotal roles in determining the efficacy of a stent. All of the testing helped explore the relative stiffness of materials, the impact on WSS and how more elastic materials can be used through smarter designs. As this form of comparison is not covered in literature, it is difficult to compare data to other experiments, yet all simulations were completed with accuracy at the forefront so the drawn analysis can be reliable and compared to prior work.

The primary purpose of the testing was to determine which materials would be able to produce optimal stents that were strong, minimised fluid impacts, and had favourable physiochemical properties to ensure their biocompatibility. Initial testing ranked cobalt chromium as the stiffest material, followed by the permanent metallic alloys and lastly the bioresorbable alloys. This was expected since resorbable materials have a low elastic modulus at the trade-off of being absorbed into the body over an extended period of time. Table 10 denotes the relative stiffness of each material when compared to cobalt chromium, indicating that no other alloy is nearly as stiff, with platinum chromium having the second highest stiffness at 83.6% of that of cobalt chromium. The permanent metallic alloys have a wide range of comparative stiffness with nitinol being the lowest at 34.1% the stiffness, and at such a low value, the thickness of the stent would need to be significantly increased to match a similar stent of cobalt chromium, potentially making it impractical for use. Similarly, the bioresorbable alloys ranged from 32% to 18.1%, meaning for designs of similar radial stiffness, the struts would have to be much larger to overcome this drawback, an impracticability in the stents design.

Table 1 contained all relevant data on the tested materials in which the young's modulus was the primary indicator of the stiffness of the material. All constituents have varying ultimate and yield strengths where the maximum equivalent stress ranged from 53 – 270 MPa and hence, materials such as tantalum which has a yield stress of 138 MPa will require superior stent designs, allowing for lower maximum stresses, so that it will not yield. Further, stents are required to have a minimum collapse pressure of at least 40 kPa [71] where it will deform by less than 10 percent of its diameter. From the data collected, more optimised stent designs conform to this requirement by being able to having a higher collapse pressure than required indicating there could be the potential to make these designs more minimalistic, even when using low yield strength materials.

The literature review in chapter 2 uncovered that material properties beyond purely mechanical values also affect the structural integrity of a stent. Many materials offer a varying range of intrinsic properties, including nitinol's shape memory effect and cobalt chromium releasing ions over time, potentially leading to localised inflammation [72]. Often when comparing stent materials, such traits are not fully


analysed, especially when they might have negative effects. An understanding of these materials and any adverse effects should be well documented and discussed. With such effects that can either improve survivability or be a detriment to health, it is imperative that materials are chosen such that they can aid in recovery and lead to increased survival rates.

One factor that was not tested explicitly was stent recoil, although it is becoming a prevalent issue with stents due to the lower occurrence of other problems from stent improvements. This loss of diameter lowers the effectiveness of the stent, placing a person at higher risk than needed due to the heightened risk of re operation. Recent studies by Ota and Kitahara [10, 11] have determined that recoil occurs to a lower extent in materials that are less stiff. Although data is limited in material types, cobalt chromium performs worse compared to platinum chromium and stainless steel. Although this requires a more thorough examination, it can be noted that less stiff materials will allow for less recoil in the short term and potentially the long term as well, making pliable materials more qualified candidates than previously thought.

From the FEA simulations, with the increasing rigidity of stents, the stiffness exhibited in the [compression, bending, and radial compression] simulations increased, this is not ideal as bending flexibility is required to be minimised for ease of implementation. This positive relationship means that it will be very difficult to achieve all three to a high degree and will be a mixture of using the correct material as well as an effective stent scaffold. The simulations showed that much of the stress was held within the stent connectors and that using more connectors will lead to less deformation. These results also demonstrate that as this is where the stress is often held, it is most likely where failure or fatigue will occur and is a key area of the stent susceptible to failure. Additional analysis into this is required to further understand how to optimise this aspect.

The initial FEA testing also determined that no material is ideal in all aspects, some materials such as tantalum, stainless steel 316L and platinum Iridium performed adequately in all aspects yet did not excel, while other materials, being cobalt chromium and platinum chromium were highly stiff, yet did not provide optimal bending. Bioresorbable alloys have a low stiffness, making their bending flexibility quite ideal, however the radial and compressional stiffness were low, meaning that premature failure and fatigue are at a heightened risk.

The multi objective optimisation process evaluated the haemodynamic performance of stents through CFD. This study used only idealised vessel behaviour that did not account for patient specific morphology, such as lesions, nor does it account for effects with drug coatings. It produced results that used the range of parameters available and generated differing types of stents throughout the process. The used code was the same as previously used by students and hence can be compared against, with the major change being a large choice of materials which was an added improvement. Their data used primarily cobalt chromium and showed an increase in HWSS and a decrease in LTAWSS. An analysis

of various stent geometries has demonstrated that beneficial FEA results are not always indicative of a low flow impact stent and in fact shows the opposite. Both HWSS and LWSS are detrimental to the patient when using a stent and as such, it is required to determine acceptable values where the risk can be kept to a minimum so that overall desired performance can be achieved. 

Through creating new stent designs with the optimisation code, the material that was chosen most frequently was tantalum, which was 5 out of 10 times. Such a choice was unexpected as the tests were to maximise radial stiffness and minimise LTAWSS and HWSS. Normally, this is done through using stiffer materials however a much more pliable material was chosen which goes against what is commonly done in literature. The results of this optimisation has led to the potential for materials that are generally not used due to their lower stiffness to be considered.

Although cobalt chromium is generally noted to be a strong candidate as a stent material, this thesis aimed to assess the viability of this and assist in determining other materials and plausible alternatives. The FEA studies assessed the strength of various metals while the second phase helped improve the structure of the stent and proved that differing materials may not necessarily lead to a decrease in CFD performance. Looking at other intrinsic properties, such as how Cobalt Chromium can release ions and can cause inflammation, the benefit in viable alternatives found by this study becomes cleared. These alloys, when used with a complementary design, will allow the stent to have sufficient radial strength, compressional stiffness and bending stiffness all while being biocompatible while also not increasing the flow impedance compared to prior stents.

6. Future Work

This thesis covered many areas in stent design and optimisation, yet certain outcomes were not explored in thorough detail and the results indicated further potential research areas. Particularly, these include looking at stent recoil, ideal value ranges for stiffness, and deeper understanding into an alloy's intrinsic properties. Additional research will allow for a more thorough understanding of the impact of materials and stent designs on a stent's performance.

Stent recoil remains a large issue for stents, where the mechanisms along with required material properties are not yet fully understood. Common thinking has been that stiffer materials would produce stents with lower amounts of recoil, although some recent studies have revealed the opposite. More testing into which materials will provide minimal recoil to maximise the efficacy and longevity of the stent is paramount as excessive recoil may lead to premature failure. Additional research into this will extend the conducted research to give a more wholistic overview of the interaction between materials choice, stent design, and stent performance.

Fatigue testing was also considered as a possible research avenue; however, this did not come to fruition as the three tests conducted simulations were deemed of greater importance. Such an experiment would help determine the life span of a stent based on the material and help define what the failing mechanism would be and where. Further, it would provide additional insight into material behaviour and assist in assessing the ideal material for a stent.

Throughout FEA testing, the objectives were to optimise the radial, compressional and bending stiffnesses. Without an acceptable value range or minimum value, it is difficult to objectively determine the applicability and usefulness of the stent design, with current notions of efficacy solely based on relative comparisons between current and previous values. Testing in the future to determine acceptable ranges will allow future experiments to understand whether a stent design will fail or succeed and how well it will function overall. This in turn will provide the framework for a stent to know if it is sufficient in all aspects and if it will be safe when implanted in the body or if certain performance parameters are excessively high.

The CFD testing was conducted with similar aims for optimisation, however, attempting to minimise LTAWSS and HWSS is a difficult task, and finding acceptable values where being below it will assist in minimising the onset of ISR, stent thrombosis and inflammation. Finding ideal values or thresholds for this will show which designs will provide optimal fluid dynamics that minimise patient risk. Further, the current upper and lower limits that are applied in Pascals have slightly changed over time and a robust definition of the limits would be beneficial.

The simulations that were executed throughout the project were done so to a high degree, however verification of the results obtained would be beneficial through comparison to bench tests for the same variable combinations. This would allow for an analysis into any inaccuracies or discrepancies that may be seen through the simulations. Such testing was planned for but was unable to occur due to COVID-19. As the stent is a small device, slight inaccuracies or effects that weren't included in the experiments could have a large effect on results in the real world. Such inaccuracies included the drug coating thickness, the drug type, blood vessel, and coating location on the stent. Considering these in future work will allow for more accurate simulations that consider all aspects.

Through the FEA analysis, it was made apparent that the bending stiffness heavily relied on the ring connectors for the rigidity of the structure. Due to this, it is possible that a multi material stent could be produced, where the rings are made of a stiffer material, while the connectors are made of a more elastic alloy. Such a design would promote both a high radial stiffness and high bending flexibility, while the compressional stiffness may be less ideal. However, the extent of these impacts may be acceptable indicating the need for further exploration. Examination here could reveal the potential for novel designs to produce positive results which could pave the way for a new generation of stents.

The project covered many aspects of how a stent material may impact performance, however, there were multiple aspects that were not able to be tested in the research timeframe. Further, completion of this thesis and analysis of its results has revealed additional research avenues that will provide a more holistic understanding of a materials role in a stent.

7. Conclusion

This report reviewed the current mechanisms of stent failure occurring both mechanically as well as in stent restenosis and stent thrombosis. The literature review explored current stent material choices and performance testing relating to these. This developed an understanding into the relationship between physical stent design and material selection, indicating their interrelation with how certain designs favour particular metal choices. Testing methodologies provided insight into obtaining practical and computational analysis for accurate design verification.

The experimental aims and objectives revolve around finding optimal materials that allow for maximal performance. The methodology allowed for an investigation into this through a twofold approach. The first revolved around both simulation and physical experimentation through multiple modes of failure including axial compression, radial compression and bending, varying both the stent's design and its construction material to provide a comprehensive understanding. The second part involved using multi objective optimisation code to generate new stent designs with the set of materials used as one of the parameters.

The results showed that cobalt chromium was the stiffest material, and a stiffness table was generated to help determine the stiffness of other materials. The multi objective optimisation code generated stent designs that were novel, while simultaneously opting for less stiff materials which was unanticipated. When this data was combined with the literature review, it was concluded that stiff materials which are often chosen may not produce stents that are optimal for the patient and their wellbeing in the short and long term. Such conclusions have paved the way for future works to examine what a true optimal stent requires and which material can fulfil this role.

8. References

1. Health, A.I.o. and Welfare, *Coronary heart disease*. 2020, AIHW: Canberra.
2. Iqbal, J., J. Gunn, and P.W. Serruys, *Coronary stents: historical development, current status and future directions*. Br Med Bull, 2013. **106**(1): p. 193-211.
3. Grech, E.D., *Percutaneous coronary intervention. I: History and development*. Bmj, 2003. **326**(7398): p. 1080-1082.
4. Bedoya, J., et al., *Effects of Stent Design Parameters on Normal Artery Wall Mechanics*. Journal of Biomechanical Engineering, 2006. **128**(5): p. 757-765.
5. Chichareon, P., et al., *Mechanical properties and performances of contemporary drug-eluting stent: focus on the metallic backbone*. Expert Rev Med Devices, 2019. **16**(3): p. 211-228.
6. Hirdes, M., et al., *In vitro evaluation of the radial and axial force of self-expanding esophageal stents*. Endoscopy, 2013. **45** 12: p. 997-1005.
7. Mori, K. and T. Saito, *Effects of stent structure on stent flexibility measurements*. Annals of Biomedical Engineering, 2005. **33**(6): p. 733-742.
8. Petrini, L., et al., *Numerical investigation of the intravascular coronary stent flexibility*. Journal of Biomechanics, 2004. **37**(4): p. 495-501.
9. Tanimoto, S., et al., *Late Stent Recoil of the Bioabsorbable Everolimus-Eluting Coronary Stent and its Relationship With Plaque Morphology*. Journal of the American College of Cardiology, 2008. **52**(20): p. 1616-1620.
10. Kitahara, H., et al., *Acute stent recoil and optimal balloon inflation strategy: an experimental study using real-time optical coherence tomography*. EuroIntervention, 2016. **12**(2): p. e190-8.
11. Ota, T., et al., *Impact of coronary stent designs on acute stent recoil*. Journal of Cardiology, 2014. **64**(5): p. 347-352.
12. Fattori, R. and T. Piva, *Drug-eluting stents in vascular intervention*. The Lancet, 2003. **361**(9353): p. 247-249.
13. Dangas, G. and F. Kuepper, *Restenosis: Repeat Narrowing of a Coronary Artery*. Circulation, 2002. **105**(22): p. 2586-2587.
14. Buccheri, D., et al., *Understanding and managing in-stent restenosis: a review of clinical data, from pathogenesis to treatment*. Journal of thoracic disease, 2016. **8**(10): p. E1150-E1162.
15. Modi, K., M.P. Soos, and K. Mahajan, *Stent thrombosis*. StatPearls [Internet], 2020.
16. Werkum, J.W.v., et al., *Predictors of Coronary Stent Thrombosis*. Journal of the American College of Cardiology, 2009. **53**(16): p. 1399-1409.
17. Mauri, L., et al., *Stent thrombosis in randomized clinical trials of drug-eluting stents*. New England journal of medicine, 2007. **356**(10): p. 1020-1029.
18. Torrado, J., et al., *Restenosis, Stent Thrombosis, and Bleeding Complications*. Journal of the American College of Cardiology, 2018. **71**(15): p. 1676-1695.
19. Kivelä, A. and J. Hartikainen, *Restenosis related to percutaneous coronary intervention has been solved?* Annals of Medicine, 2006. **38**(3): p. 173-187.
20. Lee, D.-H. and J.M.d.l.T. Hernandez, *The newest generation of drug-eluting stents and beyond*. Eur Cardiol, 2018. **13**(1): p. 54-59.
21. Sousa, J.E., W. Serruys Patrick, and A. Costa Marco, *New Frontiers in Cardiology*. Circulation, 2003. **107**(17): p. 2274-2279.
22. Chitkara, K. and A. Gershlick, *Second versus first-generation drug-eluting stents*. J Interv Cardiol, 2010. **5**: p. 23-26.
23. Indolfi, C., S. De Rosa, and A. Colombo, *Bioresorbable vascular scaffolds—basic concepts and clinical outcome*. Nature Reviews Cardiology, 2016. **13**(12): p. 719.

24. Onuma, Y., J. Ormiston, and P.W. Serruys, *Bioresorbable scaffold technologies*. Circulation Journal, 2011: p. 1102011094-1102011094.
25. Dyet, J.F., et al., *Mechanical properties of metallic stents: how do these properties influence the choice of stent for specific lesions?* Cardiovascular and interventional radiology, 2000. **23**(1): p. 47-54.
26. Ako, J., et al., *Design Criteria for the Ideal Drug-Eluting Stent*. The American Journal of Cardiology, 2007. **100**(8, Supplement 2): p. S3-S9.
27. Rogers, C.D., *Drug-eluting stents: role of stent design, delivery vehicle, and drug selection*. Reviews in cardiovascular medicine, 2002. **3**(S5): p. 10-15.
28. Palmaz, J.C., et al., *Influence of stent design and material composition on procedure outcome*. Journal of Vascular Surgery, 2002. **36**(5): p. 1031-1039.
29. Kobayashi, Y., et al., *Long-term vessel response to a self-expanding coronary stent: a serial volumetric intravascular ultrasound analysis from the ASSURE trial*. Journal of the American College of Cardiology, 2001. **37**(5): p. 1329-1334.
30. Gundert, T.J., et al., *Optimization of Cardiovascular Stent Design Using Computational Fluid Dynamics*. Journal of Biomechanical Engineering, 2012. **134**(1).
31. Malek, A.M., S.L. Alper, and S. Izumo, *Hemodynamic Shear Stress and Its Role in Atherosclerosis*. JAMA, 1999. **282**(21): p. 2035-2042.
32. Kapoor, D., *Nitinol for Medical Applications: A Brief Introduction to the Properties and Processing of Nickel Titanium Shape Memory Alloys and their Use in Stents*. Johnson Matthey Technology Review, 2017. **61**: p. 66-76.
33. Kukreja, N., et al., *The future of drug-eluting stents*. Pharmacological Research, 2008. **57**(3): p. 171-180.
34. Hanawa, T., *Materials for metallic stents*. Journal of Artificial Organs, 2009. **12**(2): p. 73-79.
35. Marrey, R.V., et al., *Fatigue and life prediction for cobalt-chromium stents: A fracture mechanics analysis*. Biomaterials, 2006. **27**(9): p. 1988-2000.
36. Kapnis, K., et al., *Multi-scale mechanical investigation of stainless steel and cobalt–chromium stents*. Journal of the Mechanical Behavior of Biomedical Materials, 2014. **40**: p. 240-251.
37. O'Brien, B.J., et al., *A platinum–chromium steel for cardiovascular stents*. Biomaterials, 2010. **31**(14): p. 3755-3761.
38. Di Mario, C., et al., *Drug-eluting bioabsorbable magnesium stent*. Journal of interventional cardiology, 2004. **17**(6): p. 391-395.
39. Mostaed, E., et al., *Zinc-based alloys for degradable vascular stent applications*. Acta Biomater, 2018. **71**: p. 1-23.
40. Bowen, P.K., J. Drelich, and J. Goldman, *Zinc exhibits ideal physiological corrosion behavior for bioabsorbable stents*. Advanced materials, 2013. **25**(18): p. 2577-2582.
41. Bowen, P.K., et al., *Evaluation of wrought Zn–Al alloys (1, 3, and 5 wt% Al) through mechanical and in vivo testing for stent applications*. Journal of Biomedical Materials Research Part B: Applied Biomaterials, 2018. **106**(1): p. 245-258.
42. Black, J., *Biologic performance of tantalum*. Clinical Materials, 1994. **16**(3): p. 167-173.
43. Jaschke, W., K. Klose, and E. Strecker, *A new balloon-expandable tantalum stent (Strecker-Stent for the biliary system: Preliminary Experience*. Cardiovascular and interventional radiology, 1992. **15**(6): p. 356-359.
44. Mani, G., et al., *Coronary stents: a materials perspective*. Biomaterials, 2007. **28**(9): p. 1689-1710.
45. McGrath, D.J., et al., *Nitinol stent design – understanding axial buckling*. Journal of the Mechanical Behavior of Biomedical Materials, 2014. **40**: p. 252-263.
46. Chua, S.D., B. Mac Donald, and M. Hashmi, *Finite-element simulation of stent expansion*. Journal of Materials Processing Technology, 2002. **120**(1-3): p. 335-340.

47. Gong, X.-Y., et al. *Finite element analysis and experimental evaluation of superelastic Nitinol stent*. in *SMST 2003: International Conference on Shape Memory and Superelastic Technologies*. International Organization on SMST, Pacific Grove, CA. 2004.
48. Wu, W., et al., *An FEA method to study flexibility of expanded coronary stents*. Journal of Materials Processing Technology, 2007. **184**(1-3): p. 447-450.
49. Karanasiou, G.S., et al., *Stents: Biomechanics, Biomaterials, and Insights from Computational Modeling*. Ann Biomed Eng, 2017. **45**(4): p. 853-872.
50. Everett, K.D., et al., *Structural mechanics predictions relating to clinical coronary stent fracture in a 5 year period in FDA MAUDE database*. Annals of biomedical engineering, 2016. **44**(2): p. 391-403.
51. *Nitinol - NiTi Shape Memory Alloy; High-Temperature Phase*. 2021 [cited 2021 15/04/21]; Available from: <http://www.matweb.com/search/DataSheet.aspx?MatGUID=de9dd08433714f698d513766dccea437&ckck=1>.
52. AZoM. *Stainless Steel - Grade 316 (UNS S31600)*. 2021 [cited 2021 15/04/21]; Available from: <https://www.azom.com/article.aspx?ArticleID=863>.
53. *Cobalt Chromium Alloy*. 2021 [cited 2021 15/04/21]; Available from: <https://www.americanelements.com/cobalt-chromium-alloy>.
54. Idziak-Jabłońska, A., K. Karczewska, and O. Kuberska, *Modeling of mechanical phenomena in the platinum-chromium coronary stents*. Journal of Applied Mathematics and Computational Mechanics, 2017. **16**(4): p. 29-36.
55. *WE43 MAGNESIUM*. 2020 [cited 2021 15/04/21]; Available from: <https://www.smithmetal.com/we43-magnesium-alloy.htm>.
56. AZoM. *Magnesium Elektron WE43 Alloy (UNS M18430)*. 2021 [cited 2021 15/04/21]; Available from: <https://www.azom.com/article.aspx?ArticleID=9279>.
57. *Magnesium WE43-T6, Cast*. 2021 [cited 2021 15/04/21]; Available from: <http://www.matweb.com/search/datasheet.aspx?matguid=4b8a8c13cf354fc5893a40cf8eca022c&n=1>.
58. AZoM. *Magnesium AZ80 Alloy (UNS M11800)*. 2021 [cited 2021 15/04/21]; Available from: <https://www.azom.com/article.aspx?ArticleID=6709>.
59. AZoM. *Zinc-Aluminum Alloys – ZA27*. 2021 [cited 2021 15/04/21]; Available from: <https://www.azom.com/article.aspx?ArticleID=9286>.
60. *Tantalum, Ta; Annealed*. 2021 [cited 2021 15/04/21]; Available from: [matweb.com/search/datasheet.aspx?matguid=638e0acc45ad481788d5ff142b1a7e0a](http://www.matweb.com/search/datasheet.aspx?matguid=638e0acc45ad481788d5ff142b1a7e0a).
61. 2018 [cited 2021 15/04/21]; Available from: <https://www.makeitfrom.com/material-properties/90-Platinum-10-Iridium-Electrical-Contact-Alloy>.
62. *Medical Grade Stainless Steel 316LVM*. 2021 [cited 2021 15/04/21]; Available from: <http://www.matweb.com/search/datasheet.aspx?matguid=29a84d10fada4e4fa3ebe3986e52d848>.
63. Scientific, B. *REBEL™ Platinum Chromium Coronary Stent System*. 2014; Available from: <https://www.bostonscientific.com/content/dam/bostonscientific/Interventional%20Cardiology/portfolio-group/Stents/REBEL/REBEL-Metal-Composition-Letter-US-IC-228503-AA.pdf>.
64. Maleckis, K., et al., *Comparison of femoropopliteal artery stents under axial and radial compression, axial tension, bending, and torsion deformations*. Journal of the mechanical behavior of biomedical materials, 2017. **75**: p. 160-168.
65. Pelton, A., et al., *Fatigue and durability of Nitinol stents*. Journal of the mechanical behavior of biomedical materials, 2008. **1**(2): p. 153-164.
66. Frank, A.O., P.W. Walsh, and J.E. Moore Jr, *Computational Fluid Dynamics and Stent Design*. Artificial Organs, 2002. **26**(7): p. 614-621.
67. Gharleghi, R., et al., *A multi-objective optimization of stent geometries*. Journal of Biomechanics, 2021. **125**: p. 110575.

68. Luvio, V., *Multi-objective Design Optimisation of Coronary Stents*. 2020.
69. Senthurnathan, A., *Computational and Experimental Assessment of the Mechanical Performance of Stents* 2020.
70. Kumar, A., et al., *Design Methodology of a Balloon Expandable Polymeric Stent*. Journal of Biomedical Engineering and Medical Devices, 2019. **04**.
71. Blair, R.W., et al., *Multi-objective optimisation of material properties and strut geometry for poly(L-lactic acid) coronary stents using response surface methodology*. PLOS ONE, 2019. **14**(8): p. e0218768.
72. Jantzen, C., et al., *Chromium and cobalt ion concentrations in blood and serum following various types of metal-on-metal hip arthroplasties: a literature overview*. Acta orthopaedica, 2013. **84**(3): p. 229-236.
73. Chen, C., et al., *In vivo and in vitro evaluation of a biodegradable magnesium vascular stent designed by shape optimization strategy*. Biomaterials, 2019. **221**: p. 119414-119414.
74. Wei, L., et al., *Structural and Hemodynamic Analyses of Different Stent Structures in Curved and Stenotic Coronary Artery*. Front Bioeng Biotechnol, 2019. **7**: p. 366-366.
75. Mostaed, E., et al., *Novel Zn-based alloys for biodegradable stent applications: Design, development and in vitro degradation*. J Mech Behav Biomed Mater, 2016. **60**: p. 581-602.
76. Cockerill, I., et al., *Designing Better Cardiovascular Stent Materials: A Learning Curve*. Advanced functional materials, 2021. **31**(1): p. 2005361-n/a.
77. Fu, J., et al., *Evolution of metallic cardiovascular stent materials: A comparative study among stainless steel, magnesium and zinc*. Biomaterials, 2020. **230**: p. 119641-119641.
78. Gao, F., et al., *Layer-by-layer deposition of bioactive layers on magnesium alloy stent materials to improve corrosion resistance and biocompatibility*. Bioact Mater, 2020. **5**(3): p. 611-623.
79. Shen, X., et al., *Multi-Objective Optimization Design of Balloon-Expandable Coronary Stent*. Cardiovasc Eng Technol, 2019. **10**(1): p. 10-21.
80. Ng, J., et al., *Over-expansion capacity and stent design model: An update with contemporary DES platforms*. Int J Cardiol, 2016. **221**: p. 171-179.
81. Khosravi, A., et al., *A numerical study on the application of the functionally graded materials in the stent design*. Mater Sci Eng C Mater Biol Appl, 2017. **73**: p. 182-188.
82. Khurana, J.B., M. Frecker, and E.M. Pauli, *Design and Optimization of Functionally Graded Superelastic NiTi Stents*. 2020.
83. Bowen, P.K., et al., *Biodegradable Metals for Cardiovascular Stents: from Clinical Concerns to Recent Zn-Alloys*. Advanced Healthcare Materials, 2016. **5**(10): p. 1121-1140.
84. Lally, C., F. Dolan, and P.J. Prendergast, *Cardiovascular stent design and vessel stresses: a finite element analysis*. Journal of Biomechanics, 2005. **38**(8): p. 1574-1581.
85. Dvorsky, D., et al., *High strength AM50 magnesium alloy as a material for possible stent application in medicine*. Materials Technology, 2019. **34**(14): p. 838-842.
86. Lee, D.-H. and J.M. de la Torre Hernandez, *The Newest Generation of Drug-eluting Stents and Beyond*. European cardiology, 2018. **13**(1): p. 54-59.
87. Amanov, A., S.W. Lee, and Y.S. Pyun, *Low friction and high strength of 316L stainless steel tubing for biomedical applications*. Materials Science and Engineering: C, 2017. **71**: p. 176-185.
88. Cristea, D., I. Ghiuta, and D. Munteanu, *TANTALUM BASED MATERIALS FOR IMPLANTS AND PROSTHESES APPLICATIONS*. Bulletin of the Transilvania University of Braşov. Series I Engineering Sciences, 2015. **8**(2): p. 151.
89. Bhargava, B., et al., *A novel platinum-iridium, potentially gamma radioactive stent: Evaluation in a porcine model*. Catheter Cardiovasc Interv, 2000. **51**(3): p. 364-368.

9. Appendices

9.1. Appendix A

This section contains a literature table to assist in showing how useful certain articles were and what these journals entailed. Highlighted articles were especially useful in this thesis.

<u>Number</u>	<u>Paper</u>	<u>When</u>	<u>Author</u>	<u>Journal</u>	<u>Key Points</u>	<u>End Note</u> <u>X9</u>
1	Mechanical properties and performances of contemporary drug-eluting stent: focus on the metallic backbone	2019	Chichareon, Ply	Expert Rev Med Devices	<ul style="list-style-type: none"> - Materials used in stents currently(metals) - Mechanical issues ie recoil, LSD - Stent design(coil, slotted tubes, modular, helical) 	[5]
2	In vivo and in vitro evaluation of a biodegradable magnesium vascular stent designed by shape optimization strategy	2019	Chen, Chenxin	Biomaterials	<ul style="list-style-type: none"> - Degradation of stents in vivo - Explores uneven corrosion due to factors such as localised corrosion - Optimises the stents for expansion through 72 iterations - Focuses on a magnesium vascular stent that is comprised of multiple metals to allow for optimal performance in all aspects 	[73]

3	Structural and Hemodynamic Analyses of Different Stent Structures in Curved and Stenotic Coronary Artery	2019	Wei, Lingling	Front Bioeng Biotechnol	<ul style="list-style-type: none"> - Uses 6 different stent of which 3 are commercial and 3 are self designed to run testing - Tests examined dog boning, max plastic strain, largest diameter change and recoil etc - Strut thickness was kept as a constant to allow for better comparisons - There was high variations of plastic strain and OSI between the models 	[74]
4	Novel Zn-based alloys for biodegradable stent applications: Design, development and in vitro degradation	2016	Mostaed, E.	J Mech Behav Biomed Mater	<ul style="list-style-type: none"> - Goes through different materials and collects information on the corrosion rate of the materials in a substitute medium known as hanks modified solution - Detailed information on how the stents were produced - Issues were brought up on laser irradiation - The stent degradation per day must be less than the required daily intake so that excess amounts of certain metals are not absorbed. - 	[75]
5	Designing Better Cardiovascular Stent Materials: A Learning Curve	2021	Cockerill, Irsalan	Advanced functional materials	<ul style="list-style-type: none"> - Shows the current materials used for stents and the producers of them - Demonstrates the pros and cons of all generations of stents - Some degradation of polymers can cause problems, localised inflammation - Trials stents that are on the market 	[76]

6	Evolution of metallic cardiovascular stent materials: A comparative study among stainless steel, magnesium and zinc	2020	Fu, Jiayin	Biomaterials	<ul style="list-style-type: none"> - Tested degradation rates and the antibacterial property of the materials - Tests loss of strength over time - Did a three month test which measured the material, surrounding pH and hemocompatibility 	[77]
7	Layer-by-layer deposition of bioactive layers on magnesium alloy stent materials to improve corrosion resistance and biocompatibility	2020	Gao, Fan	Bioact Mater	<ul style="list-style-type: none"> - Coats a magnesium stent with various substances to explore the effect on shortcomings of the stent such as corrosion resistance - Blood compatibility is a factor for chosen materials 	[78]
8	Zinc-based alloys for degradable vascular stent applications	2018	Mostaed, Ehsan	Acta Biomater	<ul style="list-style-type: none"> - Explores zinc as a potential stent material based on its biocompatibility attributes - Re tests mechanical properties after degradation has occurred 	[39]
9	Multi-Objective Optimization Design of Balloon-Expandable Coronary Stent	2019	Shen, Xiang	Cardiovasc Eng Technol	<ul style="list-style-type: none"> - Aimed to increase flexibility and reduce longitudinal stiffness - Didn't do any hemodynamic performance modelling 	[79]
10	Over-expansion capacity and stent design model: An update with contemporary DES platforms	2016	Ng, Jaryl	International Journal of Cardiology	<ul style="list-style-type: none"> - Looks at 6 in use stents - Compares over expansion due to the size of some arteries in which this would need to be done 	[80]
11	A numerical study on the application of the functionally graded materials in the stent design	2017	Khosravi	Materials, science and engineering	<ul style="list-style-type: none"> - Looks at functionally graded materials as opposed to uniform materials - Determined that FGM's exhibited lower dog boning and had better properties 	[81]

12	Nitinol for Medical Applications: A Brief Introduction to the Properties and Processing of Nickel Titanium Shape Memory Alloys and their Use in Stents	2017	Kapoor	Johnson Matthey Technology Review	<ul style="list-style-type: none"> - Explains the properties of nitinol and why it is a suitable stent material candidate - Used in self expanding stents 	[32]
13	Stents: Biomechanics, Biomaterials, and Insights from Computational Modelling	2017	Karanasiou	Ann Biomed Eng	<ul style="list-style-type: none"> - Explores the different biomechanics of stent materials - Assesses multimodal analysis of fatigue so that it is more accurate - Gives stent characteristics that are desirable - 	[49]
14	Design and Optimization of Functionally Graded Super elastic NiTi Stents	2020	Khurana	ASME 2020 International Design Engineering Technical Conferences and Computers and Information in Engineering Conference	<ul style="list-style-type: none"> - Uses a hourglass FGM nitinol in a FEA 	[82]
15	Biodegradable Metals for Cardiovascular Stents: from Clinical Concerns to Recent Zn-Alloys	2016	Bowen	Advanced Healthcare Materials	<ul style="list-style-type: none"> - Shows challenges proposed by biodegradable stents 	[83]
16	Cardiovascular stent design and vessel stresses: a finite element analysis	2005	Lally	Journal of Biomechanics	<ul style="list-style-type: none"> - Runs FEA on two stents - Shows stress and other variables on the stents - Also did tensile stress - Limitations due to modelling of the artery and the lack of bending and stress concentrations - Lack of shearing force 	[84]
17	High strength AM50 magnesium alloy as a material for possible stent application in medicine	2019	Dvorsky	Materials Technology	<ul style="list-style-type: none"> - Looks at AM50 alloy as a potential material for stent design - Tests it against straight similar materials to see which performs best 	[85]

18	The Newest Generation of Drug-eluting Stents and Beyond	2018	Lee	European Cardiology	<ul style="list-style-type: none"> - Shows what the ideal DES will have - Shows current stents and their corresponding properties. 	[86]
19	Low friction and high strength of 316L stainless steel tubing for biomedical applications	2017	Amanov	Materials science and engineering	<ul style="list-style-type: none"> - Uses UNSM method to make the nanostructure - Used 3 point bending - This method increased the strength and wear resistance of 316L SS 	[87]
20	TANTALUM BASED MATERIALS FOR IMPLANTS AND PROSTHESES APPLICATIONS	2015	D.Cristea	Bulletin of the Transilvania University of Braşov. Series I Engineering Sciences	<ul style="list-style-type: none"> - Demonstrates issues with other metals and imaging - Demonstrates tantalum as a good choice for stent material 	[88]
21	Materials for metallic stents	2009	Hanawa	Journal Of Artifical Organs	<ul style="list-style-type: none"> - Shows current metals for stents - Demonstrates strengths and weaknesses - Slightly outdated 	[34]
22	A platinum–chromium steel for cardiovascular stents	2010	O’Brien	Biomaterials	<ul style="list-style-type: none"> - Designs a platinum alloy - Checks various properties - Compares to different materials - Explains the production process 	[37]
23	A Novel Platinum-Iridium, Potentially Gamma Radioactive Stent	2000	Bhargava	Catheter Cardiovascular Intervention	<ul style="list-style-type: none"> - Assesses platinum iridium as a stent material - In conjunction with Medtronic - Finds it very biocompatible (is currently in use in DES stent) 	[89]
24	Coronary heart disease	2020	Australian Institute of Health Welfare	N/A	<ul style="list-style-type: none"> - Stats for CAD in AUS 	[1]
25	Coronary stents: historical development, current status and future directions	2013	Iqbal	Br Med Bull	<ul style="list-style-type: none"> - Gives a historical account of stents and the generations. - Gives large events that shaped the growth of stents 	[2]

26	Drug eluting stents in vascular intervention	2003	Fattori	The Lancet	- ISR and drug coatings used to combat common issues	[12]
27	Restenosis: repeat narrowing of a coronary artery	2002	Dangas	Circulation	- ISR - Methods to counteract this	[13]
28	Restenosis related to percutaneous coronary intervention has been solved?	2006	Kivela	Annals of Medicine	- ISR and drug eluting stents - Modern challenges that remain	[19]
29	Understanding and managing in-stent restenosis: a review of clinical data, from pathogenesis to treatment	2016	Buccheri	Journal Of Thoracic Medicine	- ISR and stent recoil - Restenosis statistics - Common complications	[14]
30	New Frontiers in Cardiology	2003	Sousa	Circulation	- DES technology - Provides emerging concepts	[21]
31	The newest generation of drug-eluting stents and beyond	2018	Lee	Eur Cardiol	- Development of both drugs used and designs to find an optimal solution	[20]
32	The future of drug-eluting stents	2008	Kukreja	Pharmacological Research	- Explored DES and their future - Recapped on their downfalls	[33]
33	Fatigue and life prediction for cobalt-chromium stents: A fracture mechanics analysis	2006	Marrey	Biomaterials	- Fatigue requirements for stents - Pitfalls in such requirements - How it should be completed	[35]
34	Multi-scale mechanical investigation of stainless steel and cobalt–chromium stents	2014	Kapnisis	Journal of the Mechanical Behavior of Biomedical Materials	- Examines stents in use for mechanical performance - Provide	[36]
35	In vitro evaluation of the radial and axial force of self-expanding esophageal stents	2013	Hirdes	Endoscopy	- Evaluation of radial and axial forces in stents in use	[6]
36	Effects of Stent Structure on Stent Flexibility Measurements	2005	Mori	Annals Of Biomedical Engineering	- Deep insight into which factors affect stent bending performance - Used four point bending to increase accuracy	[7]

37	Numerical investigation of the intravascular coronary stent flexibility	2004	Petrini	Journal Of Biomechanics	- Examines stent flexibility	[8]
38	Effects of Stent Design Parameters on Normal Artery Wall Mechanics	2006	Bedoya	Journal Of Biomechanical Engineering	- Stent design and the stress factors in Wall shear stress - Studies restenosis	[4]
39	Second versus first-generation drug-eluting stents	2010	Chitkara	J Interv Cardiol	- Examines the change between first and second generational stents, key differences and why it happened	[22]
40	Bioresorbable vascular scaffolds—basic concepts and clinical outcome	2016	Indolfi	Nature Reviews Cardiology	- Basics into Bioresorbable alloys and their fundamental concepts, what they aim to achieve and why	[23]
41	Bioresorbable scaffold technologies	2011	Onuma	Circulation Journal	- Explains why they are used	[24]
42	Finite element analysis and experimental evaluation of superelastic Nitinol stent	2004	Gong	SMST 2003: International Conference on Shape Memory and Superelastic Technologies. International Organization on SMST, Pacific Grove, CA	- Issues with nitinol FEA testing - Assumed a non linear FEA	[47]
43	An FEA method to study flexibility of expanded coronary stents	2007	Wu	Journal of Materials Processing Technology	- Uses FEA to examine bending stiffness of certain stent designs	[48]
44	Nitinol stent design – understanding axial buckling	2014	McGrath	Journal of the Mechanical Behavior of Biomedical Materials	- Investigates axial buckling during crimping	[45]
45	Finite-element simulation of stent expansion	2002	Chua	Journal of Materials Processing Technology	- Examined stents during initial stent expansion using FEA - Seems to be one of the first to do such simulations	[46]
46	Comparison of femoropopliteal artery stents under axial and radial compression, axial tension, bending, and torsion deformations	2017	Maleckis	Journal of the Mechanical Behavior of Biomedical Materials	- Examines deformation in much modes - Recent paper	[64]
47	Drug-eluting bioabsorbable magnesium stent	2004	Di Mario	Journal of interventional cardiology	- Explores magnesium-based stent design	[38]

					- Uses interesting design	
48	Mechanical properties of metallic stents: how do these properties influence the choice of stent for specific lesions?	2000	Dyet	Cardiovascular and interventional radiology	- Examines balloon expandable and self-expanding stents for radial force, radio-opacity, trackability and flexibility	[25]
49	Design Criteria for the Ideal Drug-Eluting Stent	2007	Ako	The American Journal of Cardiology	- Analyses Drug eluting stents and what can be improved on them - Explores the properties that an ideal stent would have	[26]
50	Drug-eluting stents: role of stent design, delivery vehicle, and drug selection	2002	Rogers	Reviews in cardiovascular medicine	- Focus on stent design, delivery vehicle and drug properties - Defines the design as a choice between acute procedural success and long term biological stability	[27]
51	Influence of stent design and material composition on procedure outcome	2002	Palmaz	Journal of Vascular Surgery	- Examines the impact on stents on healing, thrombotic, inflammatory and hyperplastic responses	[28]
52	Long-term vessel response to a self-expanding coronary stent: a serial volumetric intravascular ultrasound analysis from the ASSURE trial	2001	Kobayashi	Journal of the American College of Cardiology	- Explores radial size over a period of time to minimise vessel wall injury	[29]
53	Zinc exhibits ideal physiological corrosion behaviour for bioabsorbable stents	2013	Bowen	Advanced materials	- Examines zinc as a potential material for stents	[40]
54	Evaluation of wrought Zn–Al alloys (1, 3, and 5 wt% Al) through mechanical and in vivo testing for stent applications	2018	Bowen	Journal of Biomedical Materials Research Part B: Applied Biomaterials	- Uses a zinc aluminium alloy as a potential stent material - Analyses strength	[41]
55	Biologic performance of tantalum	1994	Black	Clinical Materials	- Detailed piece on tantalum and its biological performance - Old paper	[42]
56	A new balloon-expandable tantalum stent (Strecker-Stent for	1992	Jaschke	Cardiovascular and interventional radiology	- Explores balloon dilation with a specific stent and 30 patients	[43]

	the biliary system: Preliminary Experience					
57	Coronary stents: a materials perspective	2007	Mani	Biomaterials	- Explores materials currently used in coronary stents - Slightly old	[44]
58	Modeling of mechanical phenomena in the platinum-chromium coronary stents	2017	Idziak-Jabłońska	Journal of Applied Mathematics and Computational Mechanics	- Stent analysis based on compression - Uses a platinum and chromium alloy	[54]
59	Percutaneous coronary intervention. I: History and development	2003	Grech	Bmj	- Gives a historical account of stents	[3]
60	Stent thrombosis	2020	Modi	StatPearls [Internet]	- Defines stent thrombosis - Good initial insight into this problem	[15]
61	Predictors of Coronary Stent Thrombosis	2009	Jochem	Journal of the American College of Cardiology	- Attempts to find predictors of thrombosis	[16]
62	Stent thrombosis in randomized clinical trials of drug-eluting stents	2007	Mauri	New England journal of medicine	- Uses clinical trials for data, using 878 patients	[17]
63	Restenosis, Stent Thrombosis, and Bleeding Complications	2018	Torrado	Journal of the American College of Cardiology	- Examines restenosis, thrombosis and bleeding - Reports causes	[18]
64	Structural mechanics predictions relating to clinical coronary stent fracture in a 5 year period in FDA MAUDE database	2016	Everett	Annals of biomedical engineering	- Examines stent fracture - Very few examine this	[50]
65	Fatigue and durability of Nitinol stents	2008	Pelton		- Examines fracture in nitinol stents - Gives data and causes	[65]
66	Design Methodology of a Balloon Expandable Polymeric Stent	2019	Kumar	Journal Of Biomedical Engineering and Medial Devices	- Showed Design process of a polymer based stent	[70]
67	Multi-objective optimisation of material properties and strut geometry for poly(L-lactic acid)	2019	Blair	PLOS ONE	- Optimization Parameters	[71]

	coronary stents using response surface methodology					
68	Impact of Coronary Stent Designs on Acute Stent Recoil	2014	Ota	Journal of Cardiology	- Stent recoil in both the short and long term	[11]
69	Acute stent recoil and optimal balloon inflation strategy: an experimental study using real-time optical coherence tomography	2016	Kitahara	EuroIntervention	- Stent Recoil Over time	[10]
70	Chromium and cobalt ion concentrations in blood and serum following various types of metal-on-metal hip arthroplasties: a literature overview	2013	Jantzen	Acta orthopaedica	- Explored issues with cobalt chromium used in the body	[72]
71	Optimization of Cardiovascular Stent Design Using Computational Fluid Dynamics	2012	Gundert	Journal Of Biomedical Engineering	- Explains how CFD simulations are run for stents	[30]
72	Hemodynamic Shear Stress and Its Role in Atherosclerosis	1999	Malek	JAMA	- Explores problem due to WSS	[31]
73	Computation Fluid Dynamcis and Stent Design	2002	Frank	Artificial Organs	- Explores the basics of CFD and stents	[66]
74	A multi-Objective optimisation of stents	2021	Gharlegghi	Journal of Biomechanics	- Multi Objective Design - CFD	[67]
75	Late Stent Recoil of the Bioabsorbable Everolimus-Eluting Coronary Stent and its Relationship With Plaque Morphology	2008	Tanimoto	Journal of the American college of Cardiology	- Stent recoil	[9]

9.2. Appendix B

The following tables denote the stiffness values for the tested stents in all materials and all simulations.

Table 12. Stiffness Values for Nitinol, SS 316L and Cobalt Chromium for all Simulations

Stiffness	Nitinol			SS 316L			Cobalt Chromium		
	Bending	Comp	Radial	Bending	Comp	Radial	Bending	Comp	Radial
1	0.221594	4.93E-03	624.2142	0.518016	0.011509	1453.815	0.649422	0.014457	1828.248
2	0.185934	2.68E-03	1141.097	0.436537	0.006296	2657.63	0.545595	0.007873	3342.084
3	0	0	0	0	0	0	0	0	0
4	0.348585	5.69E-03	858.5068	0.815818	0.013293	1999.2	1.021932	0.016675	2514.337
5	0.733152	4.78E-02	1002.28	1.7098	0.111164	2332.031	2.147239	0.139868	2934.725
6	0.776435	1.82E-02	1579.723	1.823444	0.042446	3674.386	2.277774	0.053281	4625.112
7	0.219049	5.51E-03	555.8357	0.512567	0.012905	1292.907	0.642271	0.016165	1627.294
8	0.306857	7.67E-03	2270.488	0.717378	0.017928	5281.148	0.899469	0.022492	6647.284
9	0	0	0	0	0	0	0	0	0
10	0.180707	5.50E-03	304.3535	0.422712	0.012878	707.9292	0.529786	0.016127	891.0282
11	1.081737	1.90E-02	1985.579	2.528917	0.044332	4618.52	3.170599	0.055624	5813.307
12	0	0	0	0	0	0	0	0	0
13	0.248862	7.20E-03	588.3797	0.582576	0.016869	1368.732	0.72987	0.021122	1722.617
14	2.786593	1.74E-01	959.0946	6.504541	0.405312	2232.121	8.159636	0.509009	2808.393
15	0.661861	1.88E-02	1654.242	1.548799	0.044015	3849.783	1.940603	0.055089	4843.81
16	0.311753	1.55E-02	909.2159	0.726498	0.036125	2114.295	0.912935	0.045466	2661.694
17	0.060005	7.75E-04	572.7553	0.140159	0.001809	1333.131	0.175691	0.002272	1677.16
18	0.055579	1.13E-03	136.127	0.129902	0.002649	317.4818	0.162921	0.003323	398.8645
19	0.109785	1.99E-03	434.1387	0.257206	0.004666	1011.152	0.32195	0.005841	1271.495
20	0.313813	5.49E-03	1259.995	0.73486	0.012876	2931.311	0.919959	0.01612	3689.133
21	0.619281	2.84E-02	637.6475	1.442592	0.066113	1483.991	1.813406	0.083193	1867.131
22	1.122514	5.59E-02	731.4667	2.621003	0.130338	1704.238	3.288295	0.163882	2142.527
23	0.324349	7.58E-03	1025.831	0.760001	0.017721	2386.789	0.951352	0.022219	3003.629
24	0.377567	7.26E-03	1974.508	0.885273	0.017018	4592.824	1.107613	0.021296	5780.903
25	0.831833	9.59E-03	2029.927	1.94868	0.022487	4726.022	2.439642	0.028137	5944.59
26	2.485601	1.03E-01	3882.467	5.794333	0.240833	9040.823	7.277639	0.302663	11370.51
27	5.729268	1.78E-01	4.20E+03	13.3443	0.414683	9756.09	16.75492	0.521673	12287.69
28	0.868359	1.68E-02	1109.811	2.031421	0.039344	2585.069	2.545386	0.049196	3250.52
29	8.942559	3.05E-01	1443.51	20.87187	0.709351	3357.449	26.16565	0.892866	4226.169
30	0	0	0	0	0	0	0	0	0
31	2.633759	1.24E-01	2625.707	6.14171	0.289638	6102.873	17.52405	0.364281	21522.87
32	6.013611	2.53E-01	4081.876	14.01441	0.589905	9484.81	17.5989	0.742065	11947.21
33	4.463953	1.95E-01	2727.108	10.4061	0.452767	6339.378	13.06656	0.569676	7982.909
34	4.004719	2.45E-01	7286.348	9.342848	0.571121	16939.05	11.72492	0.718443	21329.56
35	5.018692	1.99E-01	3301.993	11.69916	0.463537	7692.54	14.69212	0.582727	9671.724
36	5.426769	2.00E-01	7519.144	12.64246	0.466935	17470.12	15.88032	0.587225	22007.47

Table 13. Stiffness Values for Platinum Chromium, Mg(WE34) and Zinc-Magnesium for all simulations

Stiffness	Platinum Chromium			Mg(WE43)			Zinc-Magnesium		
	Bending	Comp	Radial	Bending	Comp	Radial	Bending	Comp	Radial
1	0.543038	0.012083	1527.634	0.118082	0.002623	331.3523	0.127144	0.00284	360.5607
2	0.456496	0.006586	2792.544	0.099443	0.001433	605.7209	0.106046	0.001531	659.307
3	0	0	0	0	0	0	0	0	0
4	0.854664	0.01394	2100.865	0.185937	0.003028	455.6632	0.199683	0.003266	496.0749
5	1.794864	0.11686	2451.83	0.389858	0.02534	531.5898	0.42213	0.027586	579.772
6	1.906135	0.044537	3863.897	0.415525	0.009671	837.624	0.442521	0.010451	914.064
7	0.537092	0.013518	1359.461	0.11679	0.002939	294.7229	0.125538	0.003155	321.9895
8	0.752082	0.018803	5553.22	0.163486	0.004084	1203.876	0.17608	0.004406	1314.796
9	0	0	0	0	0	0	0	0	0
10	0.443013	0.013487	744.3721	0.096325	0.002933	161.3747	0.103602	0.003145	176.3442
11	2.65116	0.0465	4856.535	0.576363	0.0101	1052.835	0.620667	0.010899	1149.299
12	0	0	0	0	0	0	0	0	0
13	0.61035	0.017664	1439.114	0.132714	0.003841	312.0034	0.142547	0.004119	340.7893
14	6.822746	0.425437	2346.357	1.483743	0.092355	508.7873	1.601816	0.099957	554.9085
15	1.622834	0.046075	4046.875	0.352914	0.010022	877.5172	0.37928	0.010731	957.2772
16	0.763007	0.037985	2223.528	0.165653	0.008235	481.9851	0.179718	0.008975	526.7849
17	0.146936	0.001899	1401.253	0.031977	0.000412	303.8658	0.034449	0.000446	331.4222
18	0.136214	0.002778	333.3473	0.029601	0.000603	293.8127	0.031911	0.000651	320.2554
19	0.269293	0.004885	1062.422	0.058609	0.001063	230.4542	0.062804	0.001138	250.9784
20	0.769505	0.013482	3082.04	0.167508	0.002932	668.2008	0.17961	0.003143	729.2326
21	1.515478	0.069506	1559.947	0.328926	0.015071	338.2596	0.357205	0.016414	368.9613
22	2.749287	0.136942	1790.319	0.597604	0.029706	388.4	0.645152	0.032273	422.5855
23	0.795724	0.018577	2509.383	0.173143	0.004037	544.0688	0.185522	0.004347	593.5554
24	0.92652	0.017812	4829.471	0.201673	0.003875	1046.975	0.215763	0.004147	1142.917
25	2.040503	0.023534	4966.846	0.44398	0.00512	1077.187	0.475947	0.005477	1173.881
26	6.083415	0.252935	9500.622	1.321504	0.054884	2060.606	1.431828	0.059534	2243.898
27	14.00905	0.435872	10264.09	3.047363	0.094523	2224.282	3.301808	0.102859	2432.436
28	2.12865	0.041155	2716.075	0.463006	0.008957	3278.991	0.497755	0.009562	589.1685
29	21.88464	0.745933	3530.58	4.765449	0.161708	765.3672	5.137916	0.176272	835.6683
30	0	0	0	0	0	0	0	0	0
31	17.52405	0.304381	17978.65	1.401019	0.066017	1391.362	1.51623	0.071787	1521.307
32	14.71269	0.620024	9979.465	3.197956	0.134462	2162.473	3.464472	0.146294	2365.78
33	10.92358	0.475966	6668.463	2.374085	0.103207	1445.251	2.57077	0.112366	1579.907
34	9.803033	0.600285	17817.71	2.131352	0.13018	3861.735	2.30383	0.141636	4220.145
35	12.28188	0.486952	8081.716	2.668707	0.105644	1753.191	2.890783	0.114707	1907.157
36	13.2752	0.490673	18382.5	2.884877	0.106426	3983.146	3.127995	0.115706	4358.254

Table 14. Stiffness values for Zinc-Aluminium, Tantalum and Platinum Iridium for all simulations

Stiffness	Zinc-Aluminium			Tantalum			Platinum Iridium		
	Bending	Comp	Radial	Bending	Comp	Radial	Bending	Comp	Radial
1	0.207307	0.004621	585.4805	0.492368	0.011004	1397.173	0.395241	0.00885	1126.812
2	0.173525	0.002504	1070.362	0.410676	0.005931	2554.815	0.32851	0.004746	2061.226
3	0	0	0	0	0	0	0	0	0
4	0.325897	0.005322	805.3333	0.773265	0.012654	1922.29	0.620117	0.010162	1550.821
5	0.686837	0.044803	940.6216	1.634788	0.106897	2246.616	1.315101	0.086149	1813.507
6	0.724393	0.01702	1482.761	1.713068	0.040498	3541.998	1.369781	0.03255	2859.192
7	0.204835	0.005151	521.8577	0.486285	0.012225	1247.709	0.390097	0.009801	1008.831
8	0.287087	0.00718	2131.524	0.682035	0.017073	5094.836	0.547527	0.013713	4117.233
9	0	0	0	0	0	0	0	0	0
10	0.169006	0.005137	285.7638	0.401299	0.012187	683.3339	0.321982	0.009767	552.6457
11	1.012011	0.017759	1863.851	2.404045	0.042233	4453.535	1.929869	0.033925	3596.774
12	0	0	0	0	0	0	0	0	0
13	0.232668	0.006727	552.3816	0.55226	0.01596	1320.558	0.442863	0.01279	1067.585
14	2.608701	0.16269	900.0907	6.200002	0.387332	2150.271	4.983036	0.311499	1736.626
15	0.618886	0.017536	1552.558	1.469112	0.041582	3709.449	1.178443	0.033308	2996.404
16	0.2922	0.01457	853.7186	0.696066	0.034777	2041.291	0.560395	0.028043	1650.471
17	0.056145	0.000726	537.5168	0.1333	0.001728	1284.261	0.107062	0.00139	1037.613
18	0.05201	0.001061	519.5291	0.123619	0.002524	1240.99	0.099283	0.002028	1002.394
19	0.102582	0.001859	407.2775	0.243216	0.00441	972.5413	0.194912	0.003533	785.2992
20	0.293275	0.005134	1182.666	0.69536	0.012178	2825.776	0.557404	0.009759	2282.351
21	0.58058	0.026653	598.4316	1.383589	0.063605	1429.725	1.114253	0.051274	1154.888
22	1.050827	0.052454	686.0484	2.498111	0.125056	1637.519	2.007523	0.100711	1321.507
23	0.303062	0.007088	962.7922	0.718598	0.016843	2300.027	0.57579	0.01352	1857.228
24	0.352654	0.006778	1853.462	0.835693	0.016071	4428.804	0.669253	0.012872	3577.003
25	0.777333	0.008954	1904.655	1.843463	0.021224	4548.79	1.477405	0.016994	3672.782
26	2.328977	0.096818	3642.21	5.543937	0.230695	8695.106	4.461273	0.185679	7016.567
27	5.368596	0.167077	3942.373	12.68383	0.398579	9425.69	10.21002	0.321182	7616.18
28	0.812049	0.015643	1041.005	1.927553	0.037053	2484.898	1.546467	0.029648	2005.133
29	8.369329	0.286146	1355.084	19.86767	0.683055	3238.215	15.96337	0.550748	2615.655
30	0	0	0	0	0	0	0	0	0
31	2.467121	0.116637	2465.735	5.869211	0.278173	5895.065	4.721331	0.224098	4763.499
32	5.634637	0.237647	3833.683	13.40721	0.566889	9167.396	10.78961	0.456773	7408.953
33	4.182126	0.182486	2560.825	9.950472	0.435417	6122.139	8.00589	0.350927	4947.016
34	3.750234	0.230083	6841.524	8.916993	0.548841	16353.06	7.169786	0.442224	13210.62
35	4.702207	0.186476	3096.859	11.19074	0.44449	7390.235	9.004999	0.357884	5961.06
36	5.085847	0.188007	7062.322	12.1057	0.448362	16888.23	9.74544	0.361189	13648.22

9.3. Appendix C

This section contains the full data for the newly generated stents and their performance.

Table 15. Stiffness and CFD values for generated stent Designs

Stent	Stiffness			CFD			INFLOW
	Bending	Comp	Radial	LWSS	HWSS	LTAWSS	
1	7.18975	0.228049	3991.518	9.650154	56.18036	22.75956	2143.004
2	0.643013	0.007308	2136.199	10.90541	42.29394	22.1322	2144.8
3	1.516909	0.071228	1522.225	4.505174	69.4029	10.61673	2145.875
4	0.026875	0.000554	732.3869	3.135556	69.58186	9.152891	2145.734
5	0.081238	0.00168	1194.564	4.941556	57.09939	12.41426	2145.102
6	0.467551	0.007616	3283.877	10.62577	43.29903	21.4677	2144.883
7	1.373511	0.060926	1594.28	6.10333	65.70155	13.78006	2145.691
8	1.092477	0.011859	3687.697	12.13937	40.60851	24.42313	2145.415
9	0.611452	0.006386	2092.287	10.00397	44.83751	20.43605	2144.122
10	10.17687	0.008431	9792.468	8.422894	45.86863	20.83358	2145.299